

AD-A084 756

BOSTON UNIV MASS DEPT OF ASTRONOMY F/G 4/1
SHORT TERM PERIODICITIES IN IONOSPHERIC TOTAL ELECTRON CONTENT.(U)
MAR 80 K H SCHATTEN, M MENDILLO F1962R-77-C-0270
ACBU-SER-III-13

UNCLASSIFIED

AFGL -TR-80-0096

NL

/ OF 1
AD
A084756

END
DATE
FILMED
6-80
DTIC

ADA 084756

AFGL-TR-80-0096

SHORT TERM PERIODICITIES IN
IONOSPHERIC TOTAL ELECTRON CONTENT

Kenneth H. Schatten and Michael Mendillo

Department of Astronomy
Boston University
725 Commonwealth Avenue
Boston, Massachusetts 02215

Annual Scientific Report No. 2
1 October 1978 - 30 September 1979

March 1980

Approved for public release; distribution unlimited.

AIR FORCE GEOPHYSICS LABORATORY
AIR FORCE SYSTEMS COMMAND
UNITED STATES AIR FORCE
HANSCOM AFB, MASSACHUSETTS 01730

DDC FILE COPY

DTIC
SERIALIZED
MAY 28 1980
A

80 5 27 203

Qualified requestors may obtain additional copies from the Defense Documentation Center. All others should apply to the National Technical Information Service.

UNCLASSIFIED

1

SECURITY CLASSIFICATION OF THIS PAGE (When Data Entered)

19 REPORT DOCUMENTATION PAGE		READ INSTRUCTIONS BEFORE COMPLETING FORM	
1. REPORT NUMBER	2. GOVT ACCESSION NO.	3. RECIPIENT'S CATALOG NUMBER	
18 AFGL TR-80-0096	AD-A084756		
4. TITLE (and Subtitle)		5. TYPE OF REPORT & PERIOD COVERED	
6 Short Term Periodicities in Ionospheric Total Electron Content		Scientific - Annual Rpt No. 2 1 Oct 1978 - 30 Sept. 1979	
7. AUTHOR(s)		6. PERFORMING ORG. REPORT NUMBER	
10 Kenneth H. Schatten and Michael Mendillo		A.C. B.U., Ser III, No. 13	
		8. CONTRACT OR GRANT NUMBER(s)	
		F 19628-77-C-0278	
9. PERFORMING ORGANIZATION NAME AND ADDRESS		10. PROGRAM ELEMENT, PROJECT, TASK AREA & WORK UNIT NUMBERS	
Astronomy Department, Boston University 725 Commonwealth Avenue Boston, Massachusetts 02215		62101 F 464304-GB	
11. CONTROLLING OFFICE NAME AND ADDRESS		12. REPORT DATE	
Air Force Geophysics Laboratory Hanscom AFB, Bedford, MA 01730 Contract Monitor: J.A. Klobuchar/PHP		11 March 1980	
14. MONITORING AGENCY NAME & ADDRESS (if different from Controlling Office)		13. NUMBER OF PAGES	
12 54		51	
		15. SECURITY CLASS. (of this report)	
		Unclassified	
		15a. DECLASSIFICATION/DOWNGRADING SCHEDULE	
16. DISTRIBUTION STATEMENT (of this Report)			
Approved for public release; distribution unlimited.			
17. DISTRIBUTION STATEMENT (of the abstract entered in Block 20, if different from Report)			
9 Annual scientific rept. no. 2, 1 Oct 78-30 Sep 79			
18. SUPPLEMENTARY NOTES			
14 ACBU-SER-III-13			
19. KEY WORDS (Continue on reverse side if necessary and identify by block number)			
Ionospheric Variability Total Electron Content F-region Day-to-Day Variability		Lunar Effects Geomagnetic Disturbance Solar-Terrestrial Relations	
20. ABSTRACT (Continue on reverse side if necessary and identify by block number)			
Short-term variability of the ionospheric F-region has been studied using total electron content (TEC) data from several North American sites. Specific attention was given to lunar-induced periodicities in TEC and to a general treatment of changes in TEC associated with variations in the height of the F-region (hmF2). In both cases, simple analytical expressions were derived from statistical analysis of the large TEC and hmF2 data bases. These relations are appropriate for updates to model predictions of average conditions			

DD FORM 1473

JAN 73

EDITION OF 1 NOV 65 IS OBSOLETE

UNCLASSIFIED

SECURITY CLASSIFICATION OF THIS PAGE (When Data Entered)

406311

Gur

UNCLASSIFIED

SECURITY CLASSIFICATION OF THIS PAGE(When Data Entered)

20. cont.

✓ during daytime hours. A study of the "geomagnetic ordering" of TEC variability showed that real-time predictive methods can reduce up to 50% of the normal variability. A preliminary analysis of solar wind sector boundary effects suggested that sector components may order some F-region variability, though the specific relations between these effects and the geomagnetic ordering results remain to be clarified. ✓

UNCLASSIFIED

SECURITY CLASSIFICATION OF THIS PAGE(When Data Entered)

TABLE OF CONTENTS

Form DD 1473.....	i
Table of Contents.....	iii
Acknowledgements.....	iv
Chapter 1. Introduction.....	
Chapter 2. Specific Periodicities, Harmonics, Beats and Associated Relations.....	
Chapter 3. The Lunar Component.....	
Chapter 4. Increase in Total Electron Content with Ionospheric Height.....	
Chapter 5. Geomagnetic Activity Related Effects.....	
Chapter 6. Solar Related Ionospheric Variability.....	
Chapter 7. Summary and Conclusions.....	
References.....	

Accession for	
NO.	
DATE	
BY	
REMARKS	
A	

ACKNOWLEDGEMENTS

All of the total electron content data used in this study were provided by the Air Force Geophysics Laboratory in cooperation with the following individuals and institutions: (a) Goose Bay (Labrador) data...personnel of Marconi Limited, (b) Sagamore Hill (Hamilton, MA) data...Mr. Chester Malik and personnel of the Air Weather Service (Detachment 2, 12th Weather Squadron), (c) Kennedy Space Flight Center (Cape Canaveral, Fla.) data...personnel of Pan American World Airways (Meteorological Division).

We gratefully acknowledge the technical guidance and the many fruitful discussions with John Klobuchar and colleagues at the Air Force Geophysics Laboratory. At Boston University, we appreciate the technical assistance of Mr. Francis Lynch (Astronomy Department) and Mr. Joseph Iuliano (Mathematics Department) and, for their careful preparation of the manuscript and figures, Ms. Barbara Schwartz and Ms. Barbara Baumgardner in the Astronomy Department.

1. INTRODUCTION

The phrase "day-to-day" variability of the ionosphere" refers to those fluctuations in an ionospheric parameter which cannot be related directly to known solar or geomagnetic disturbances. In this report, measurements of the total electron content (TEC) of the ionosphere are used to examine various aspects of F-region variability. As with any time series of data, ionospheric TEC may be categorized on the basis of the time-scale of any periodicities associated with the series (assuming long-term stationarity). The long-term periodicities ($T > \text{months}$) causing ionospheric variability (e.g., those associated with time of year or general level of solar activity) are sufficiently well understood that predictions of average TEC at a station may be made with reasonable accuracy, based upon these parameters (Llewellyn and Bent, 1973; Hawkins and Klobuchar, 1974; and Rush, 1972). Klobuchar (1979) notes that monthly mean TEC conditions can be predicted to within ± 20 percent. He suggests that much of the remaining uncertainty resides not so much with our lack of understanding of ionospheric responses, but rather with the lack of adequate solar activity predictions for long time scales.

This paper assumes that long term TEC behavior is fairly well understood. While Rishbeth and Kohl (1976) point out that some problem areas still remain, we nevertheless concentrate on shorter term periodicities and associated non-periodic (non-sinusoidal) variations of the ionosphere. Naturally, we proceed with the goal that with an increased understanding of these variations, an increased ability to predict ionospheric variability at shorter time intervals will result.

We put forth, in this paper, a number of such searches for methods to understand and to predict short term ionospheric variability. Thus, we concentrate not only on specific TEC periodicities (power at certain frequencies), but also upon methods to find relations for possible use in algorithms suitable for predictions. These will, in general, be non-periodic or quasi-periodic functions, as a strict periodicity has a fixed form which would be well-known.

2. SPECIFIC PERIODICITIES, HARMONICS, BEATS, AND ASSOCIATED RELATIONS

Although it is possible to consider ionospheric variability in alternative ways, for consistency with Bernhardt (1978) and Huang (1978), we use:

$$\text{TEC}(t) = S(t) \left\{ 1 + M(t) \right\} \quad (1),$$

where $S(t)$ is the solar diurnal variation (monthly mean prediction, for example) and $M(t)$ is an added multiplicative factor. In Bernhardt's work, $M(t)$ is the lunar influence, and, as can be seen from equation (1), it modulates the expected solar variation to give rise to a variability in TEC. We shall consider M more generally to be any modulator of TEC.

The search for short time-scale periodicities in ionospheric electron content has been considered principally by Bernhardt (1974,1978) and references therein. Among those identified were several related to the solar rotation (synodic periodicity of about 27 days); others related to diurnal harmonics coupled with the lunar period (synodic period of 29.5 days), and others referred to as an "X" group of statistically significant variations, but ones of unknown origin.

Thus, the understanding of some of the unknown periodicities associated with the ionosphere may be similar to the atomic physicists' studies of spectral lines. The fundamentals of this search may be summarized in the following way.

A strictly periodic (but non-sinusoidal) phenomenon will give rise to power at a fundamental frequency and at higher harmonics. Figure 1 shows a power spectrum of the Total Electron Content at Hamilton/Sagamore Hill

LOG
POWER

FREQUENCY SPECTRUM
HAMILTON RAW DATA 75/76

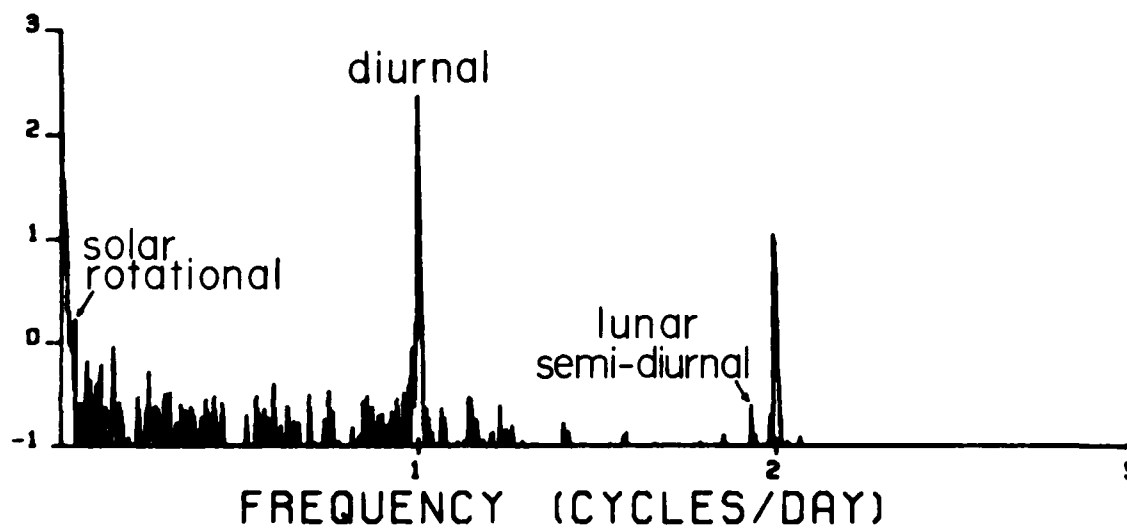


FIG. 1 Power Frequency Spectrum of the raw Hamilton
Total Electron Content for 1975-1976.

(L = 3 ionosphere) for 1975-1976 to illustrate the point. The diurnal variation is seen ($f_1 = 1$ cycle per day), with power also at the second and third harmonics. Higher harmonics are also present. It is most appropriate to think of the power at these harmonics, arising not from strict periodicities at these frequencies, but rather from the non-linear, non-sinusoidal forcing of the ionospheric TEC by the daily non-sinusoidal solar influence.

The numerous other (non-diurnal type) periodicities seen in Figure 1 may also be investigated. Let us first examine some ways these may arise. Consider a second influence on the ionosphere with an inherent periodicity described by a frequency, f_2 . In addition to it and its harmonics possibly appearing, a "beating" with other periodicities, f_1 for example, may occur. This can give rise to power at frequencies of the form, $n_1 f_1 \pm m_2 f_2$, where n_1 and m_2 are integers. These are beats of the fundamental periodicities or harmonics with each other. Table 1 lists some of these periodicities. Figure 1, for example, shows the lunar semi-diurnal harmonic at:

$$f = 2f_1 - 2f_2 = 2(1d)^{-1} - 2(29.5d)^{-1} = 1.933d^{-1} \quad (2).$$

This is the most prominent lunar harmonic as the lunar tidal influence is doubly symmetric and can be seen in Figure 1 even prior to filtering.

A continuous power spectral component may also be introduced by physical influences which are not strictly periodic. For example, ionospheric variability results from solar activity, as evidenced by the 11 year variability of TEC. Solar activity structure rotates with a synodic period near 27 days at the equator and more than 30 days at high solar latitudes. Thus, a non-discrete solar activity influence with harmonics

and beats would generate spectral power over a range of periods. In Figure 1, the solar rotational power would be near $3 \times 10^{-2} d^1$, though the period of 27 days is fairly broad-band. Most of the power located there is low-frequency power and is not resolved into a purely solar rotational component. There are also annual and longer periods present. In addition, non-discrete periodicities modulate other spectral components.

3. THE LUNAR COMPONENT

Much of the theory of lunar tides in the ionosphere were developed by Matsushita (1967), whereas Chapman and Bartels (1940) provided the main source of knowledge on the ionospheric current system and its lunar harmonics. More recently, Bernhardt (1978) developed a numerical method for separating the lunar semi-diurnal component from the solar second harmonic component. We have further studied this with the view of obtaining a simple expression for use in ionospheric models that will allow the lunar influence to be predicted.

Utilizing observations from 1975 through 1977 at the Kennedy Space Flight Center, ($L \approx 2$), Hamilton/Sagamore Hill ($L \approx 3$), and Goose Bay ($L \approx 4$), a LaGrange Multiplier technique provided a relatively simple functional form which could describe the main features of the lunar influence upon the TEC of the ionosphere. As an example of lunar filtered data, figures 2 through 4 show the KSFC lunar component in the winter (when the effect is large), while figure 5 shows some summer data when the effect nearly disappears. The disappearance of the effect in the summer may be associated with the enhanced atmospheric scale height during summer, and thus with effectively reduced height motions associated with the effect. This will be discussed in more detail below. The vertical lines in figures 2 through 5 indicate the meridian transit of the moon; these times are related to the effect, but in a complex way, insofar as the ionospheric response is also governed by an interaction with the existing ionosphere (see equation (1)).

Expressed as a fraction of the average TEC at any particular time, the fractional change due to the lunar influence ($M(t)$ in equation 1) may be

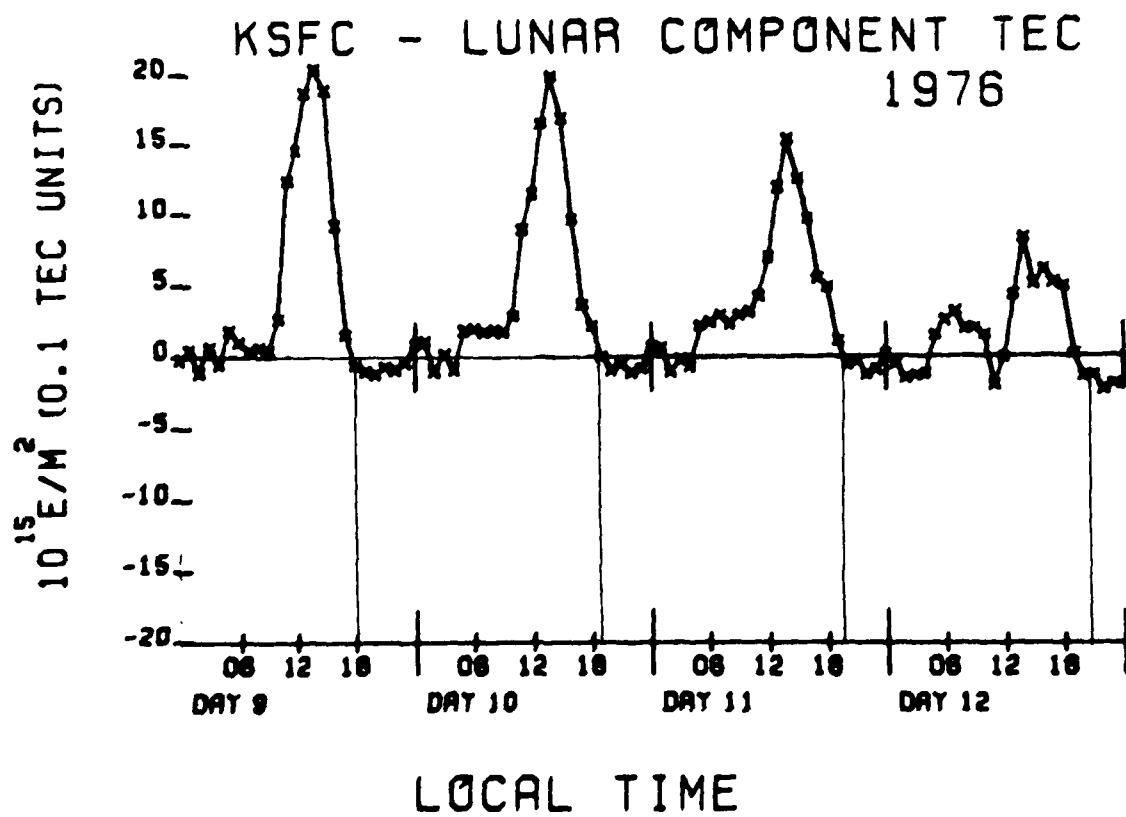


FIG. 2 Kennedy Space Flight Center lunar filtered data in tenths of a TEC unit for January 9 through 12, 1976. Note the effect is largest (nearly 2 TEC units) near midday.

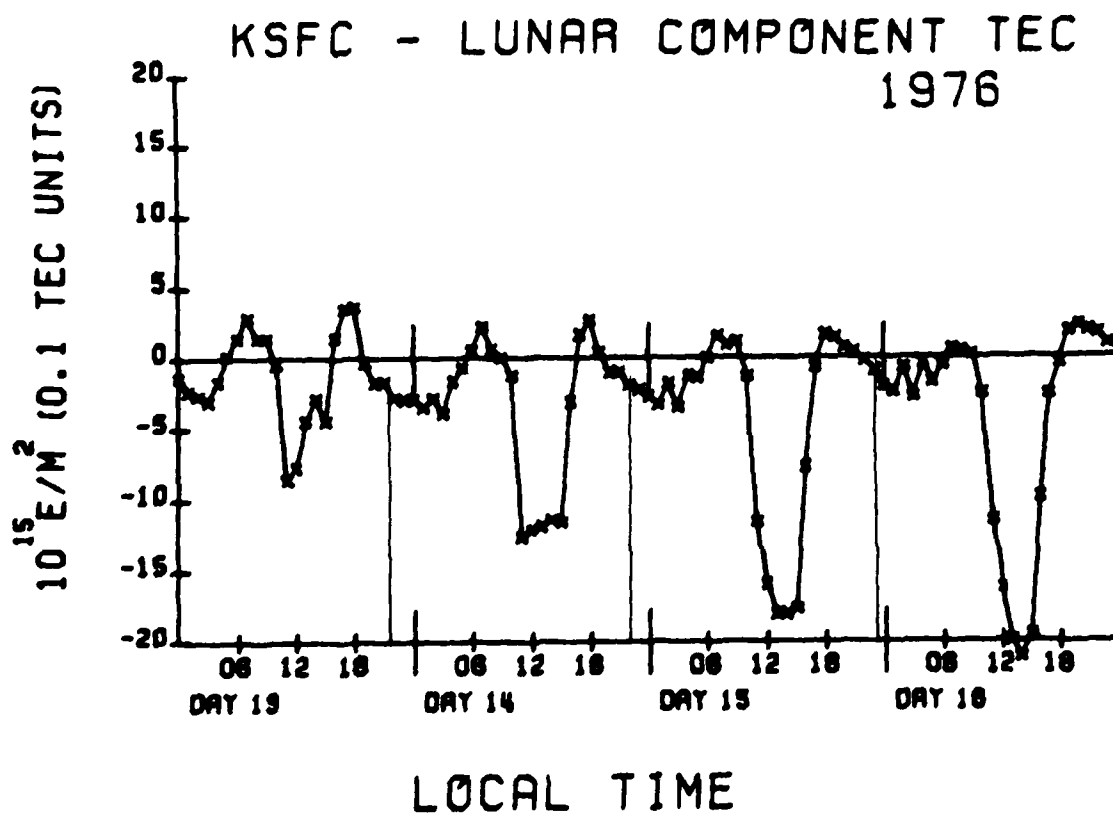


FIG. 3 Kennedy Space Flight Center lunar filtered data for January 13 through 16, 1976; the effect has now diminished and reversed as the lunar phase progresses.

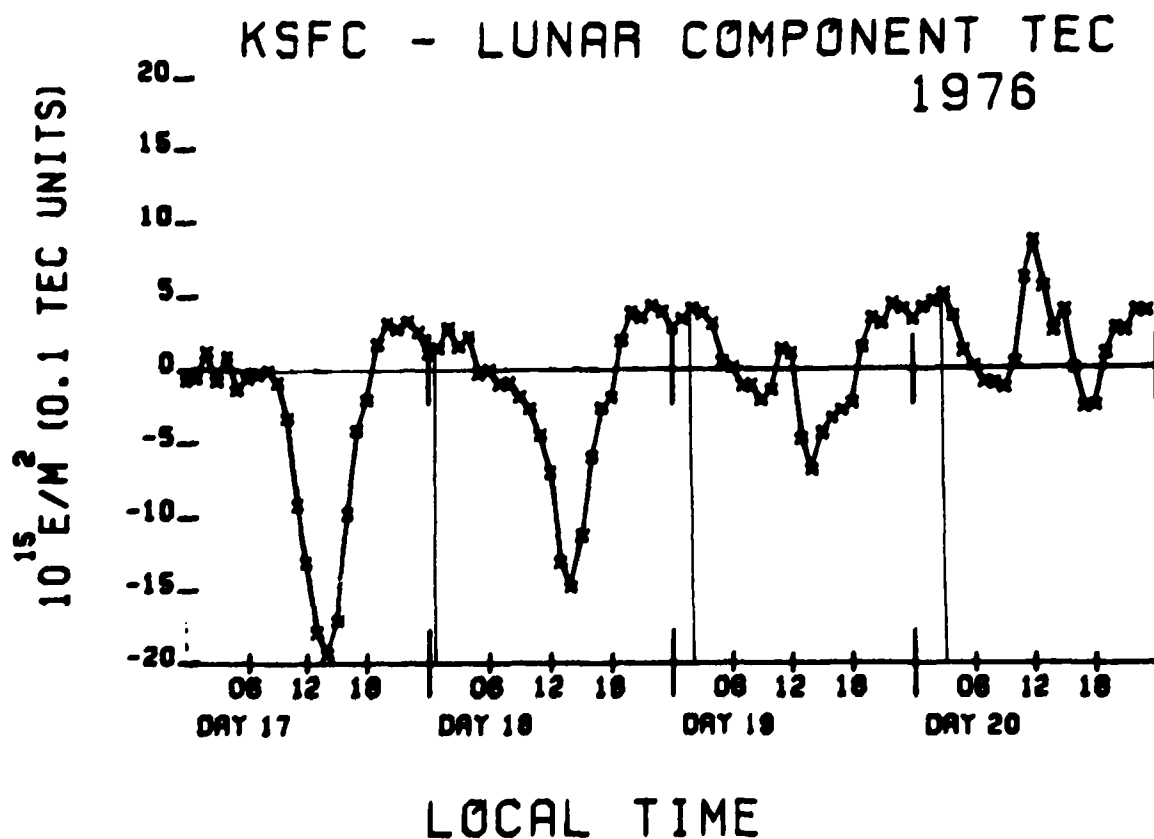


FIG. 4 Kennedy Space Flight Center lunar filtered data for January 17 through 20. The effect, now of the reverse form, is returning to the earlier sense. Full moon was on the 17th of January, 1976.

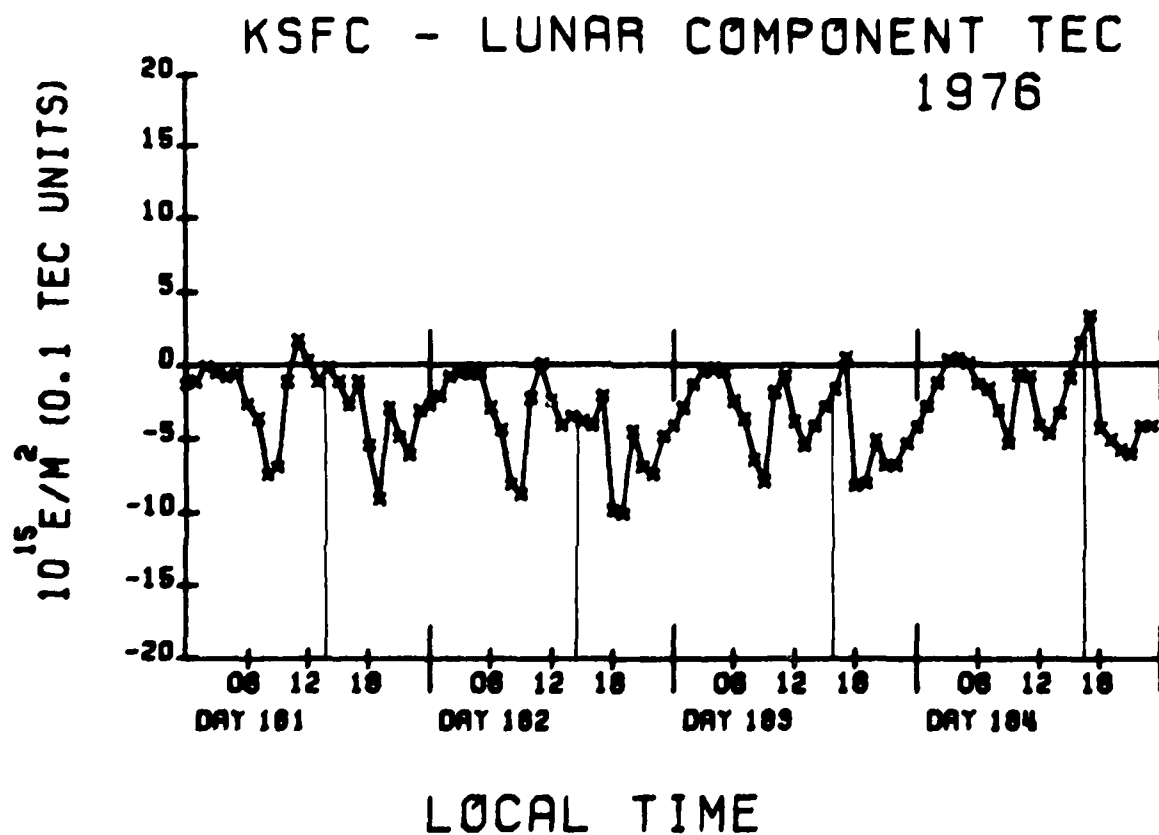


FIG. 5 Kennedy Space Flight Center lunar filtered data for days 181 through 184, 1976. Note that although the lunar meridia transit is nearly the same as in Figure 4, the effect of season markedly changes the influence; it disappears.

written as:

$$M(t) = k \times ABC \quad (3),$$

where k is a fraction depending upon the ground station, which will be discussed later. The quantities A, B , and C are normalized functions which vary in season, lunar phase, and local time, respectively. They are:

$$A = \left[\frac{1 - \sin 2 \pi (t_D - t_{VE}) / 365.25}{2} \right]^{1/4} \quad (4),$$

$$B = \cos \left[2v_L - \pi \frac{1 - 2 \pi (t_D - t_{VE}) / 365.25}{2} \right] \quad (5),$$

$$\text{and } C = \frac{\sin 5 \pi / 24 (t_s - 1300 \text{ LT})}{5 \pi / 24 (t_s - 1300 \text{ LT})} \quad (6).$$

The quantity t_D is the time in days; t_{VE} is the vernal equinox; v is lunar phase; and t_s is solar time in hours.

The functions A , B , and C are functional forms chosen to best fit the data using simple analytic expressions. The multiplicity of time scales present in these functions, and their reversal of sign, show how numerous "periodicities" or harmonics would arise from a straight power spectrum of TEC without regard to the complex behavior aspects associated with season, local time, and the non-linear forms involved.

The quantity k is station dependent. At Hamilton ($L \approx 3$ ionosphere) it is close to 0.07 (7 percent), at KSFC ($L \approx 2$ ionosphere) 0.08, and at Goose Bay ($L \approx 4$ ionosphere) 0.03. Figure 6 shows the relation of k to dip angle of the station, along with a similar plot by Bernhardt (1979).

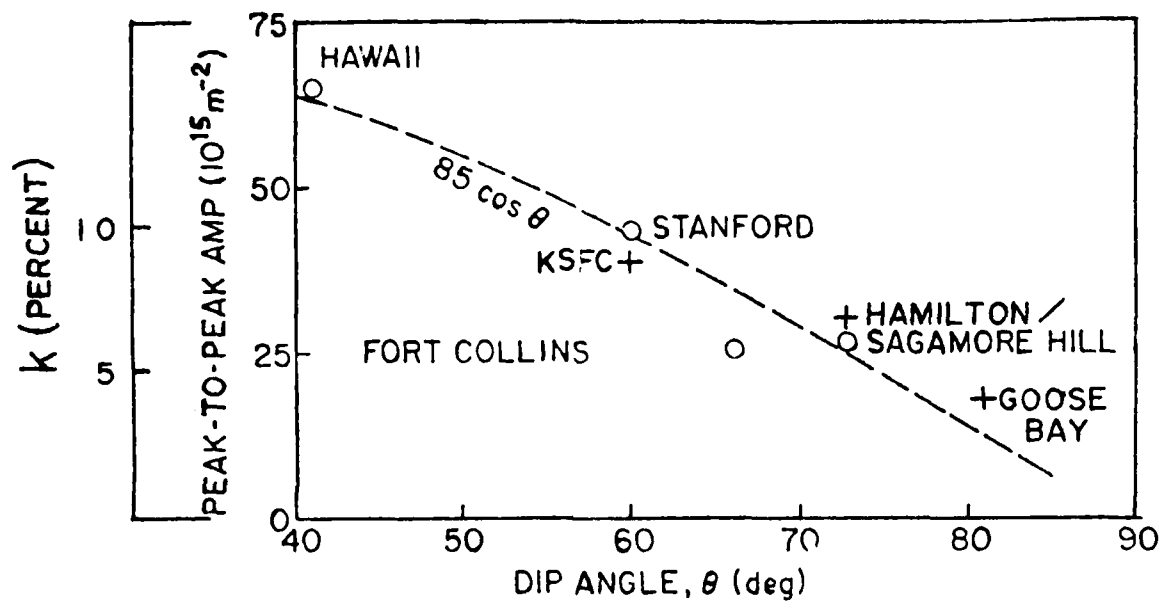


FIG. 6 Strength of the Lunar semi-diurnal component in TEC versus geomagnetic dip angle (see text).

The axis at the most left is associated with the crossed data points (this study - an average over several years), while the inner axis relates to Bernhardt's work (the circles - associated with specific data when a large peak-to-peak lunar effect occurs). The dependence upon station latitude adds support for a relation of the type where the lunar effect is given by:

$$I = C \cos \theta, \quad (7)$$

shown by the dashed curve. In Bernhardt's work, I is the peak-to-peak variation on certain days, whereas in our work it is a least-squares fit to a functional form over several years of data. In our case, I is k , and C is close to 0.2 for the three stations we used.

This relation, equation (7), is consistent with the "fountain effect" (see Bernhardt et al., 1976, and Huang, 1978), whereby lunar tidal motions have associated polarization fields resulting in an upward motion of the ionosphere by an $\underline{E} \times \underline{B}$ drift. Such a relation would provide motion roughly proportional to the cosine of the dip angle, given a nearly uniform polarization electric field. That is, if the earth's magnetic field may be written as a dipole, and a uniform eastward electric field (independent of latitude) is assumed, the resulting electrodynamic plasma drift becomes

$$V_r = \left[\frac{1}{c} \underline{E} \times \underline{B} / B^2 \right]_r = c \cos \theta. \quad (8)$$

This upward drift may result in enhanced TEC values associated with decreasing loss mechanisms through recombination, and vice versa.

Use of equation 3, and subsequent equations, has been shown to reduce TEC variability a posteriori. However, in comparison to the standard de-

viation of a monthly mean diurnal curve for TEC, the effect is not large since the above functional form has peaks only at short, limited intervals of time. Thus, the relative rareness of simultaneous peaks in A, B and C results in its limited reduction of the general TEC variability. The amplitude of nearly 1 TEC unit $\cdot (1 \times 10^{16} \text{ el/m}^2)$ in our and Bernhardt's work, however, makes it a non-negligible parameter during certain local time and seasonal periods.

4. INCREASE IN TOTAL ELECTRON CONTENT WITH IONOSPHERIC HEIGHT

The upward motion of material due to the lunar dynamo or any other cause (e.g., neutral winds) results in an increase in TEC during daylight hours (Rishbeth and Garriot, 1969; Rishbeth et al., 1978). As a way of assessing the magnitudes of such effects, we digitized the M(3000) F2 and foF2 data from Wallops Island for comparison with TEC data from Hamilton. Figures 7 through 13 are comparisons showing some preliminary results. Figures 7 and 8 show scatterplots of the total electron content of the ionosphere (ordinate) for January and February 1975 versus its corresponding hourly hmF2 value deduced from M(3000)F2, based upon Bradley's relation (1978). All local times are included in the analysis. Simple theory suggests that an increase in ionospheric height would result in a decrease in loss and thus an increase in TEC should occur. The tendency for the graphs to skew upward toward the right would suggest an influence of this kind. Figures 7 and 8 show a rather complex "butterfly" shape with one wing skewing upward to the right, and the second with a small negative slope.

If the hours chosen for analysis are restricted to daytime (1000 to 1600 LT), Figures 9 and 10 result. The lower lobe is removed and the evidence shows a TEC increase with increased hmF2. Figures 11 and 12 show the effect for April and June for daytime hours. The effect appears to diminish as summer approaches. Figure 13 shows that the effect returns during December, 1975.

The lines shown in Figures 9 through 13 are least square regression fits to the data of the form:

$$\text{TEC} = A + B * \text{hmF2} \quad (9),$$

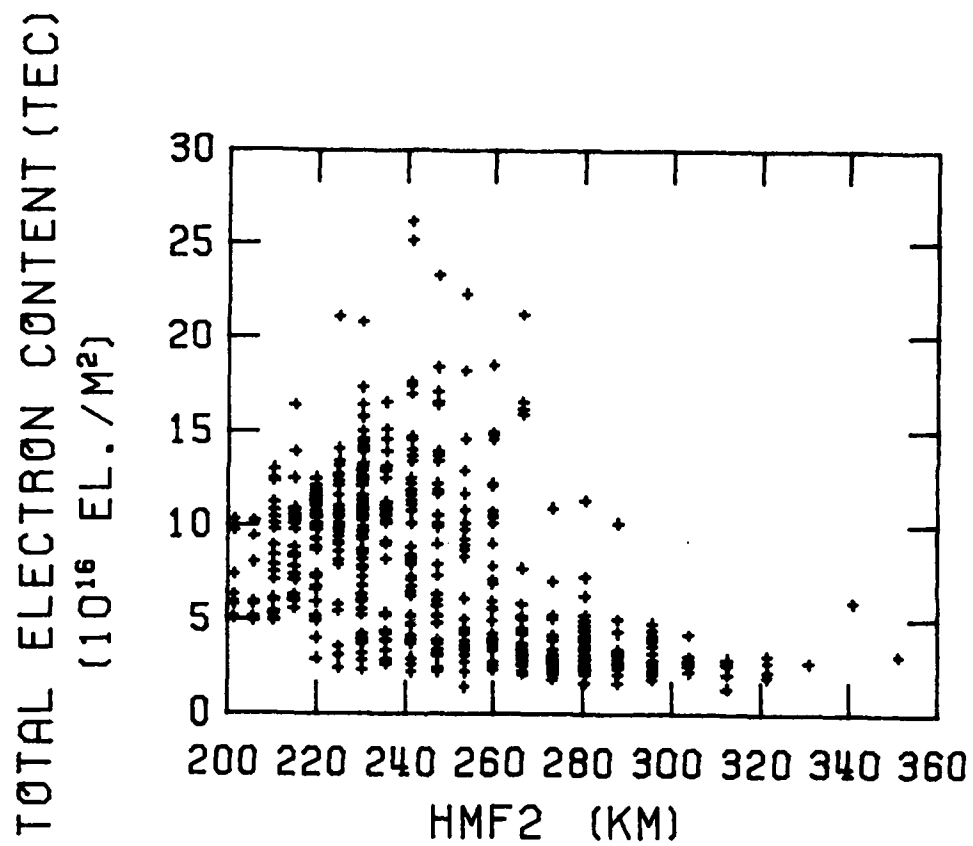


FIG. 7 Graph of hourly Total Electron Content at Hamilton vs. HmF2 based upon M(3000) F2 data from the Wallops Island ionospheric station for January, 1975.

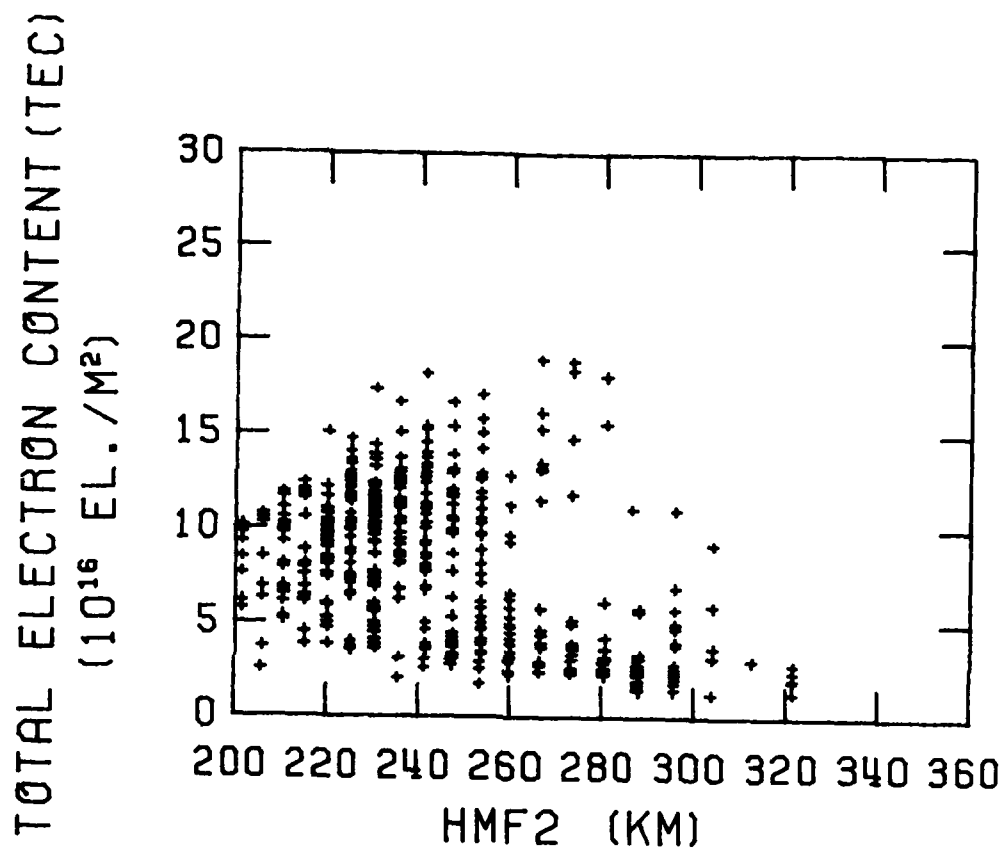


FIG. 8 Graph of hourly Total Electron Content at Hamilton vs. HmF2 based upon M(3000) F2 data from the Wallops Island ionospheric station for February, 1975.

TOTAL ELECTRON CONTENT (TEC)
(10^{16} EL./M²)

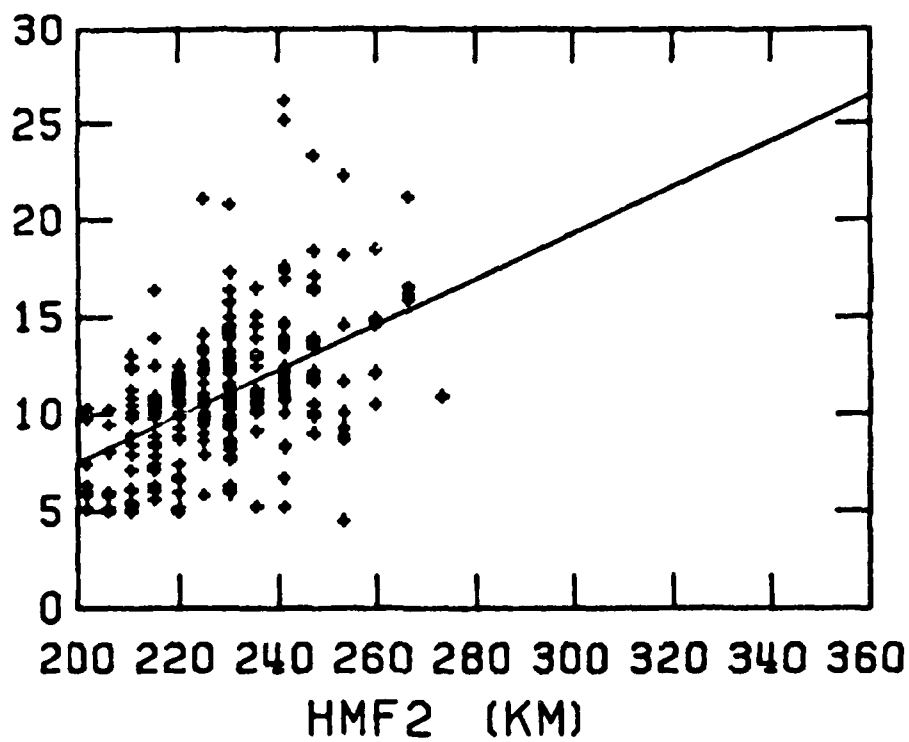


FIG. 9 Graph of hourly Total Electron Content at Hamilton vs. HmF2 during hours 1000 to 1600 LT for January, 1975.

TOTAL ELECTRON CONTENT (TEC)
(10^{16} EL./M²)

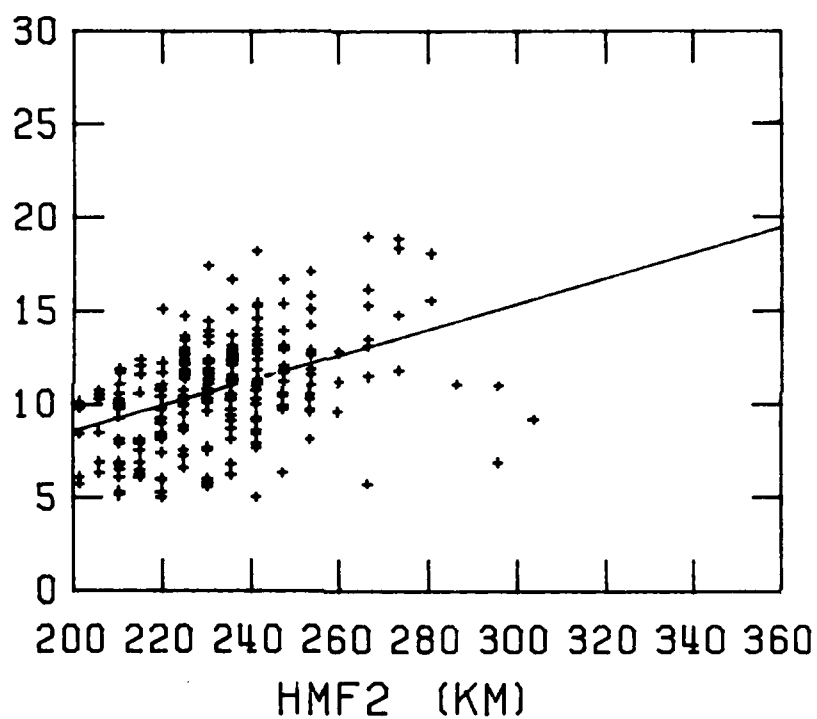


FIG. 10 Graph of hourly Total Electron Content at Hamilton vs. HmF2 during hours 1000 to 1600 LT for February, 1975.

TOTAL ELECTRON CONTENT (TEC)
(10^{16} EL./M²)

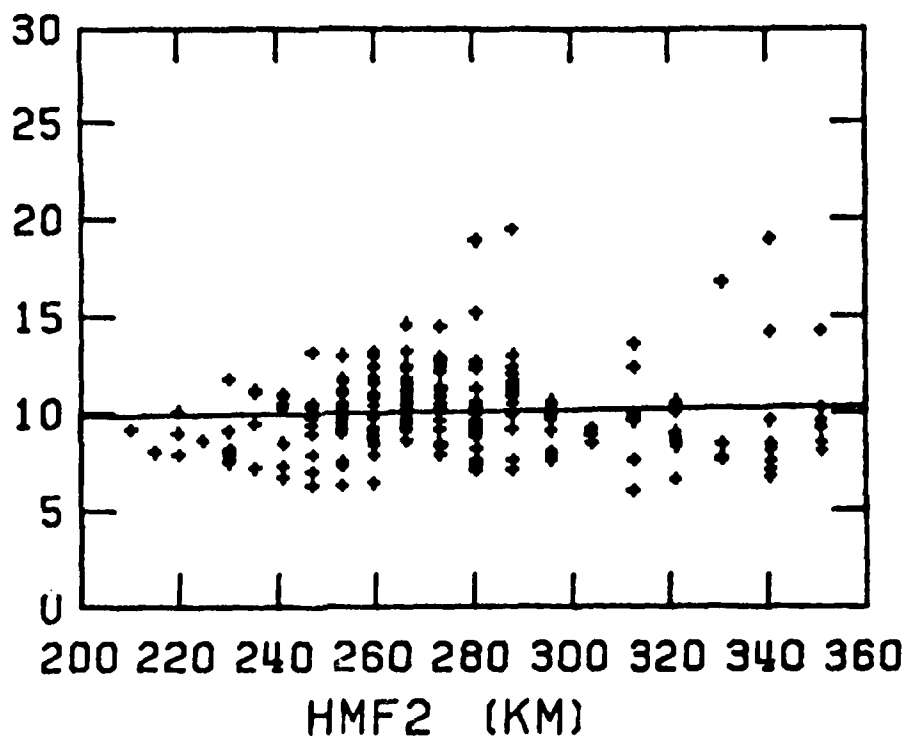


FIG. 11 Graph of hourly Total Electron Content at Hamilton vs. HmF2 during hours 1000 to 1600 LT for April, 1975.

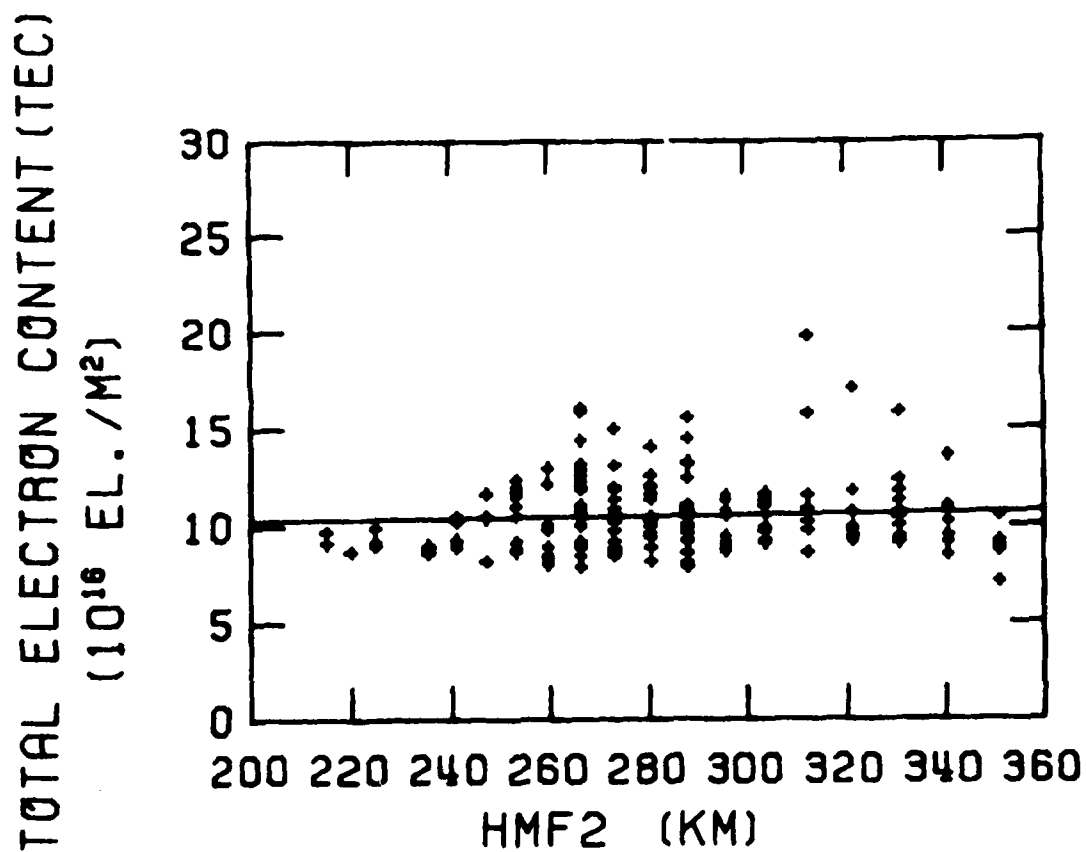


FIG. 12 Graph of hourly Total Electron Content at Hamilton vs. HmF2 during hours 1000 to 1600 LT for June, 1975.

TOTAL ELECTRON CONTENT (TEC)
(10^{16} EL./M²)

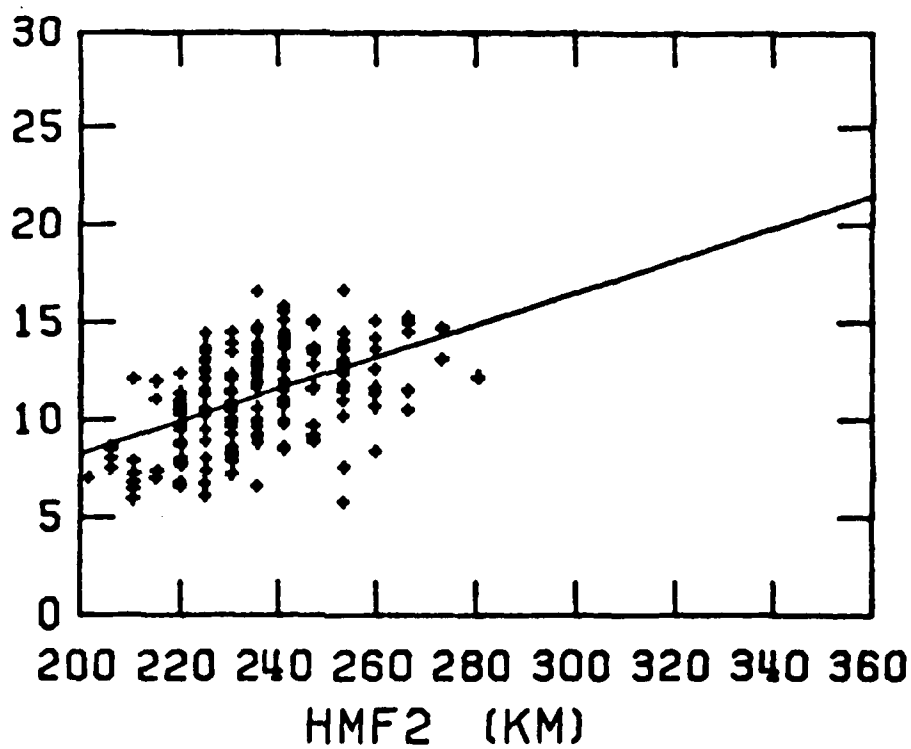


FIG. 13 Graph of hourly Total Electron Content at Hamilton vs. HmF2 during hours 1000 to 1600 LT for October, 1975.

where TEC is in 10^{16} el/m² and hmF2 in km. A clear positive regression is present for the winter and disappears in the summer. The January 1975 result, for example, is:

$$\text{TEC} = -16 + 0.118 \text{ hmF2(km)} \quad (10);$$

and thus for hmF2 at 260 km, $\overline{\text{TEC}} \sim 14.6$.

The results for 1975 at Hamilton may be synthesized with the following equation (in TEC units and hmF2 in km):

$$\overline{\text{TEC}} \approx 10.8 + \frac{(\text{hmF2} - 230)}{40} \left[1 - \sin^2 (t - t_{\text{VE}})/365.25 \right] \quad (11),$$

where $t - t_{\text{VE}}$ is time from the vernal equinox (in days).

To examine the relation of this to the lunar effect, we looked at hmF2 and TEC with a broad bandpass filter that could pick out periods from 12 to 18 days. Thus, we ourselves would not be preferentially choosing the lunar period. A ~40 km variation was observed in hmF2 and $\Delta\text{TEC} \sim 1.5 - 2$ units during winter, with the phase and frequencies closely associated with the lunar tidal motions. The above numbers represent the amplitude of a sine wave fitted to that form; the "peak-to-peak" values are twice as great.

Utilizing equation 10 with the lunar 15-day variations allows an examination of how the lunar tidal influence relates closely to other height variations. We found a ~40 km hmF2 variation, corresponding to approximately 4 in TEC units at winter solstice. This is in approximate agreement with the 1.5 - 2 value calculated with the broad bandpass filter. The difference may be explained by considering that equation (11) is based on hourly variations, whereas the lunar effect is ordered with a 15-day period.

Finally, it is worthwhile to note that both in this study and in the lunar study, the effect of vertical motions (tidal or atmospheric) upon the daytime

ionosphere was to increase the TEC when an upward motion of the ionosphere occurred, and that in both studies the largest effects appear to occur during winter months.

5. GEOMAGNETIC ACTIVITY RELATED EFFECTS

The 27-day periodicity and 11-year variation in ionospheric variability provide good indicators that solar and geomagnetic activity affect ionospheric variability. As mentioned in the introduction, Klobuchar (1979) has suggested that much of the uncertainty in long term variability resides in our inability to predict solar activity rather than a lack of our inherent knowledge about the ionospheric response. Thus, section 5.1 discusses a method whereby real-time observations may be used in a predictive mode for short-term variability. Section 5.2 deals with other possible solar related influences.

5.1 GEOMAGNETIC-ORDERING METHOD FOR PREDICTING F-REGION BEHAVIOR

A method has been developed utilizing geomagnetic variability that is moderately successful at "predicting" real-time F-region behavior. As will be seen, the method depends critically upon the similarity of the response functions to geomagnetic activity as described by Mendillo and Lynch (1979).

Figure 14, taken from Mendillo and Lynch (1979), shows the geomagnetically quiet (QQ-days) and geomagnetically disturbed (DD-days) behavior of F-region variability; we shall refer to this as "geomagnetic ordering". The "out-of-phase" or "mirror image" pattern in Figure 14 is crucial to this method. Operationally, the real-time predictive scheme could be used as follows:

- 1) define monthly mean and associated percent standard deviation at two sites (A and B); these represent state-of-the-art predictions for the F-region.
- 2) real time values at A are compared with the control curve at A

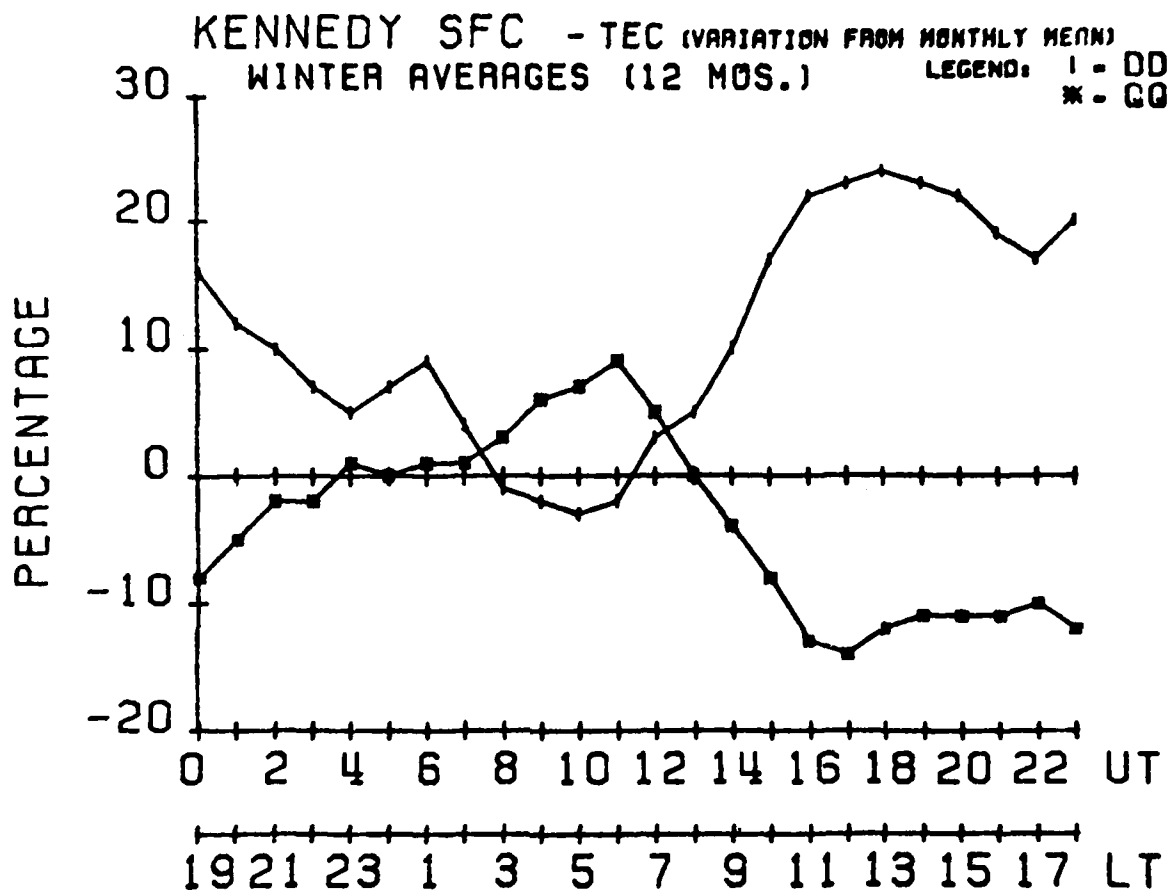


FIG. 14 Average diurnal behavior of TEC (%) for the QQ-days and DD-days for winter months at KSFC (L^2).

in order to determine if it is DD-like, QQ-like, or within some $\epsilon(\%)$ of the predicted behavior.

3) the behavior at B is then predicted to be the control curve at B updated by f_{DD} or $f_{QQ}(\%)$, or the uncorrected control curve at B. Thus, at any given hour, one of 3 values may be postulated for the behavior at B.

4) this procedure is carried out hour-by-hour for the month, and the new resultant standard deviations at B are compared with the actual data cases at B.

For illustration purposes, we considered two separate ways to test this scheme.

5.1a Method 1

As an initial test, station A's observations (at the Kennedy Space Flight Center) were divided into three classifications: QQ-like, DD-like, or "average" based upon whether the TEC variation was less than -0.43σ , near zero, or exceeded $+0.43\sigma$ of the expected hourly variation for that time period (this divides the data into thirds assuming a normal Gaussian distribution, and thus the mean of wings falls at $\sim 0.7\sigma$).

Sagamore Hill was taken to be station B, and its expected monthly mean TEC was altered by -0.7σ , 0, or $+0.7\sigma$ based on its geomagnetic ordering, for example, whether the hour in question was QQ-like, average, or DD-like at A. Figures 15 through 18 show improvements in Sagamore Hill's "forecast" based on this technique for four months in 1975. In each figure, the top curve shows the average daily TEC variation (in units of 10^{16} electrons/m², along with standard deviations throughout the day (error bars). Superposed on these are (usually) reduced standard deviations (bracketted error bars) which

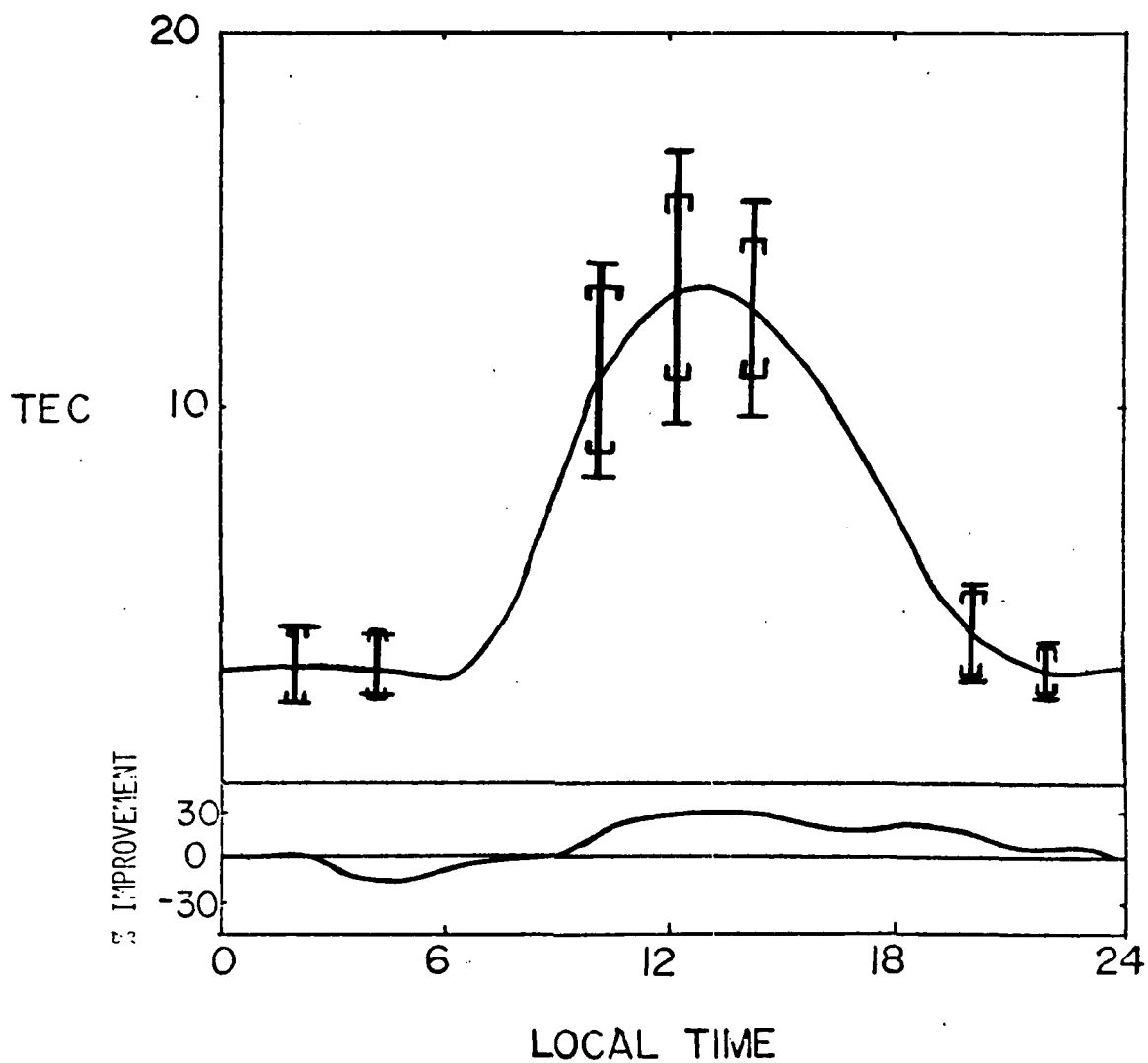


FIG. 15 Average January, 1975 TEC for Hamilton/Sagamore Hill vs. local time with standard deviations about several sample hours shown (ordinary error bars). Superimposed are bracketted error bars showing the reduction in standard deviation associated with using the "forecast" described in method 5.1a.

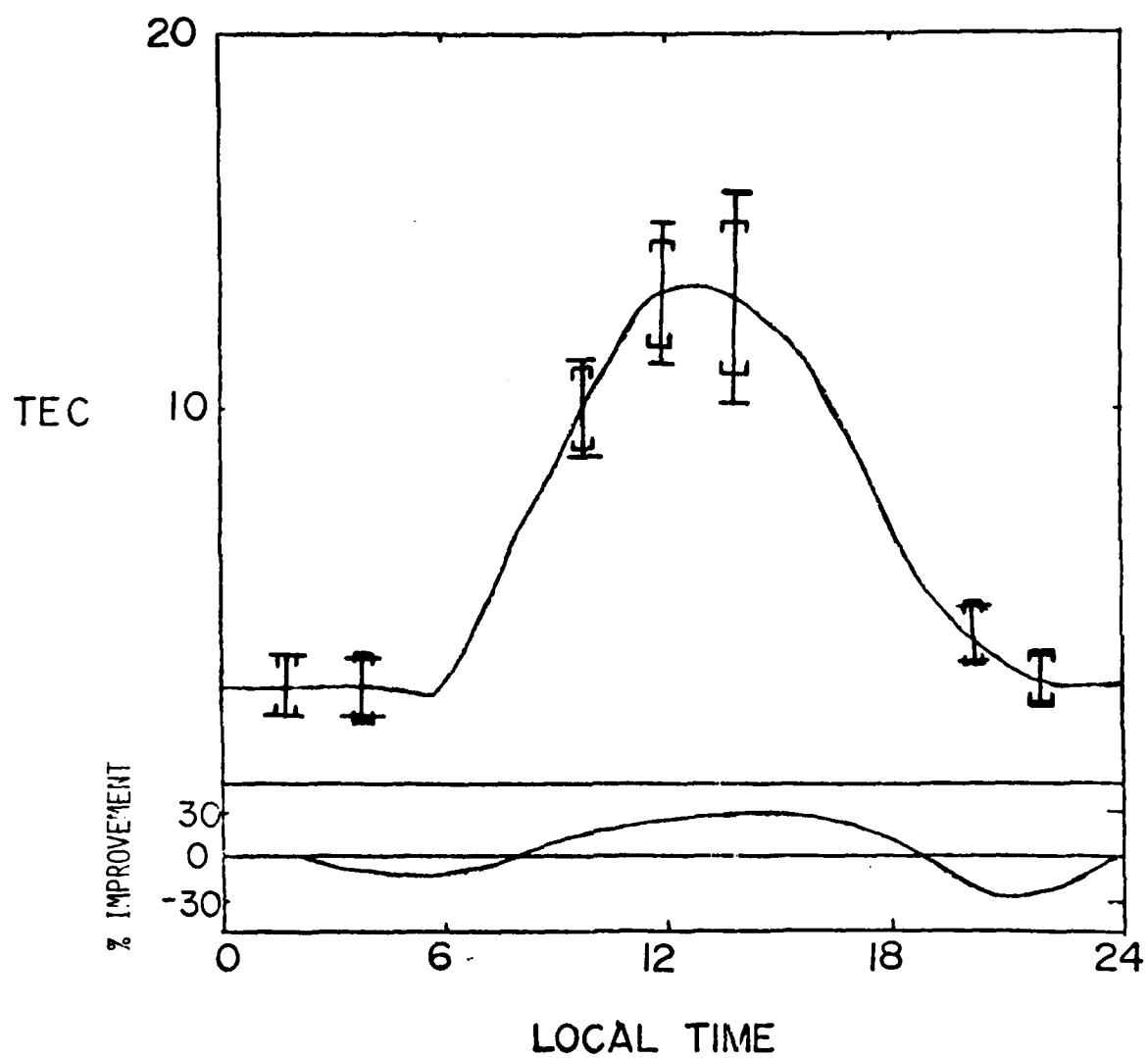


FIG. 16 Same as Figure 15 but for February, 1975.

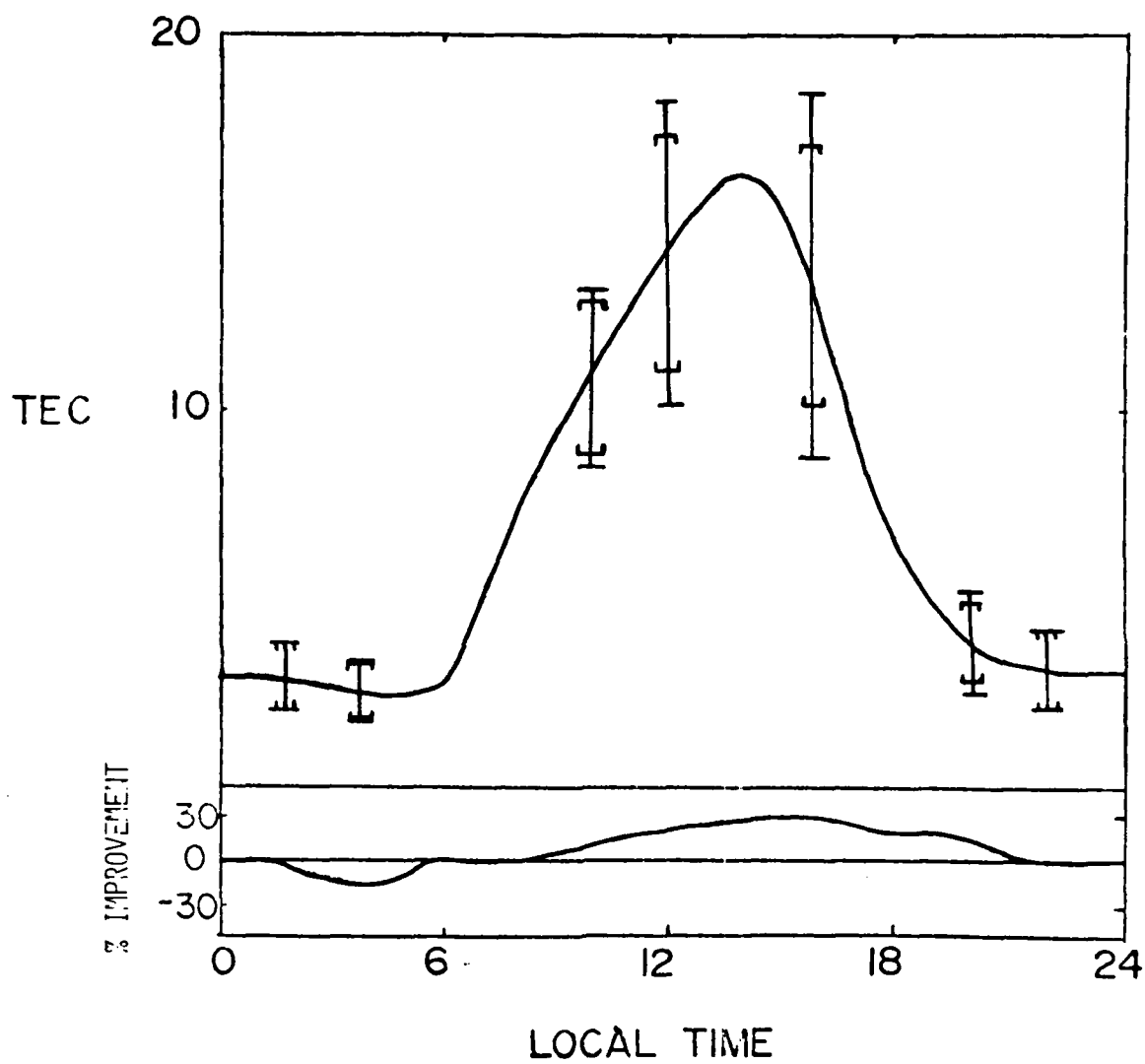


FIG. 17 Same as Figure 15 but for November, 1975.

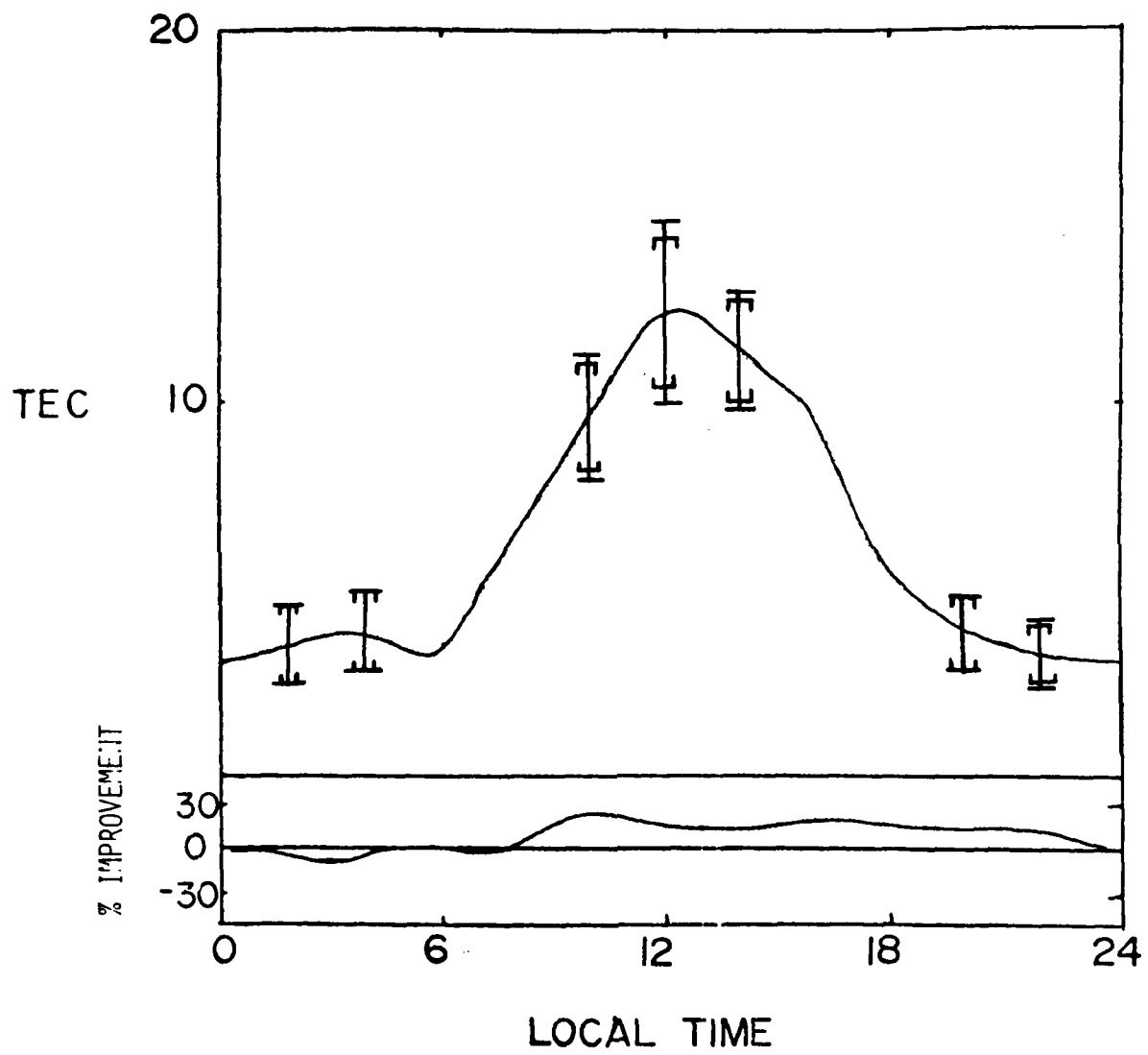


FIG. 18 Same as Figure 15 but for December, 1975.

display the reduced variations associated with removing the "forecast" based on the QQ-like or DD-like hourly behavior. The lower curve is the percent improvement throughout the day. The largest improvements occur during daylight hours.

5.1b Method 2

In the second method, a continuous function of the QQ-like or DD-like behavior is employed. Rather than dividing the geomagnetic behavior into 3 distinct quantized indices, a continuous measure is employed. The results are shown in Figures 19 through 22. A near 50% improvement in reducing the standard deviation is found. The value of this technique appears to be significant; nevertheless, the technique raises a series of questions concerning specific modes of implementation. For example, the spatial consistency of DD or QQ ordering patterns are not well known.

In order to attempt to answer this type of concern, we used KSFC as Station A and Goose Bay as Station B. The results, shown in Figure 23, yield no improvement. The reasons for this probably lie in the character of Goose Bay's "geomagnetic ordering" curves (see Figure 24): the nighttime behavior is not symmetrical about the zero axis, while the daytime curves have small amplitudes. Thus, since geomagnetic ordering is not well-defined at Goose Bay, short term prediction of these two stations, by this method, becomes virtually impossible. Hamilton's response (Figure 25), for example, was similar to KSFC's.

Part of the agreement found in the real time geomagnetic prediction technique undoubtedly results from spatial coherence of the F-region. Rush (1972, 1976) found spatial "correlations" (in NmF2) of 0.7 in the North-South direction and larger correlations at similar distances in the East-West direction.

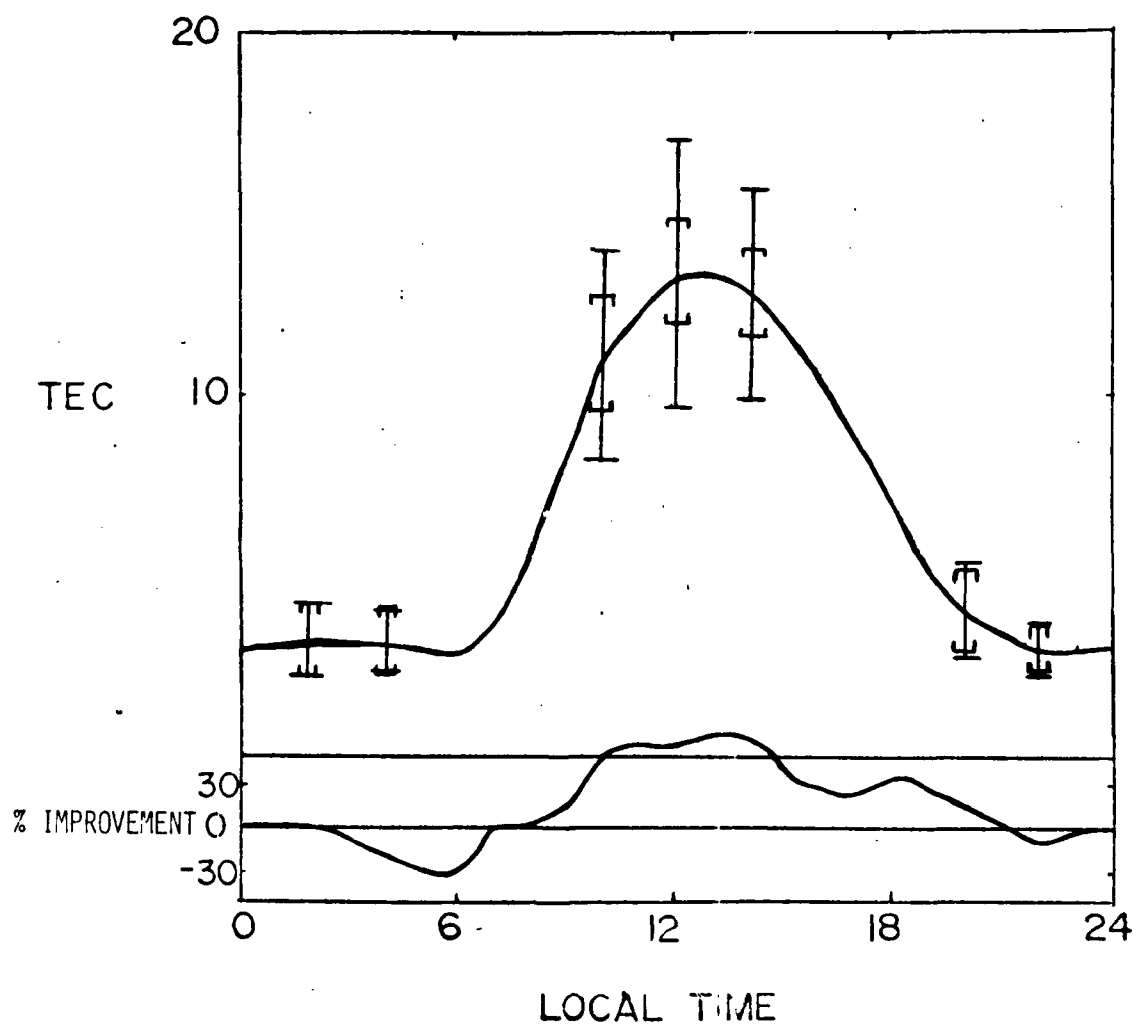


FIG. 19 Same as Figure 15 but using method 5.1b.

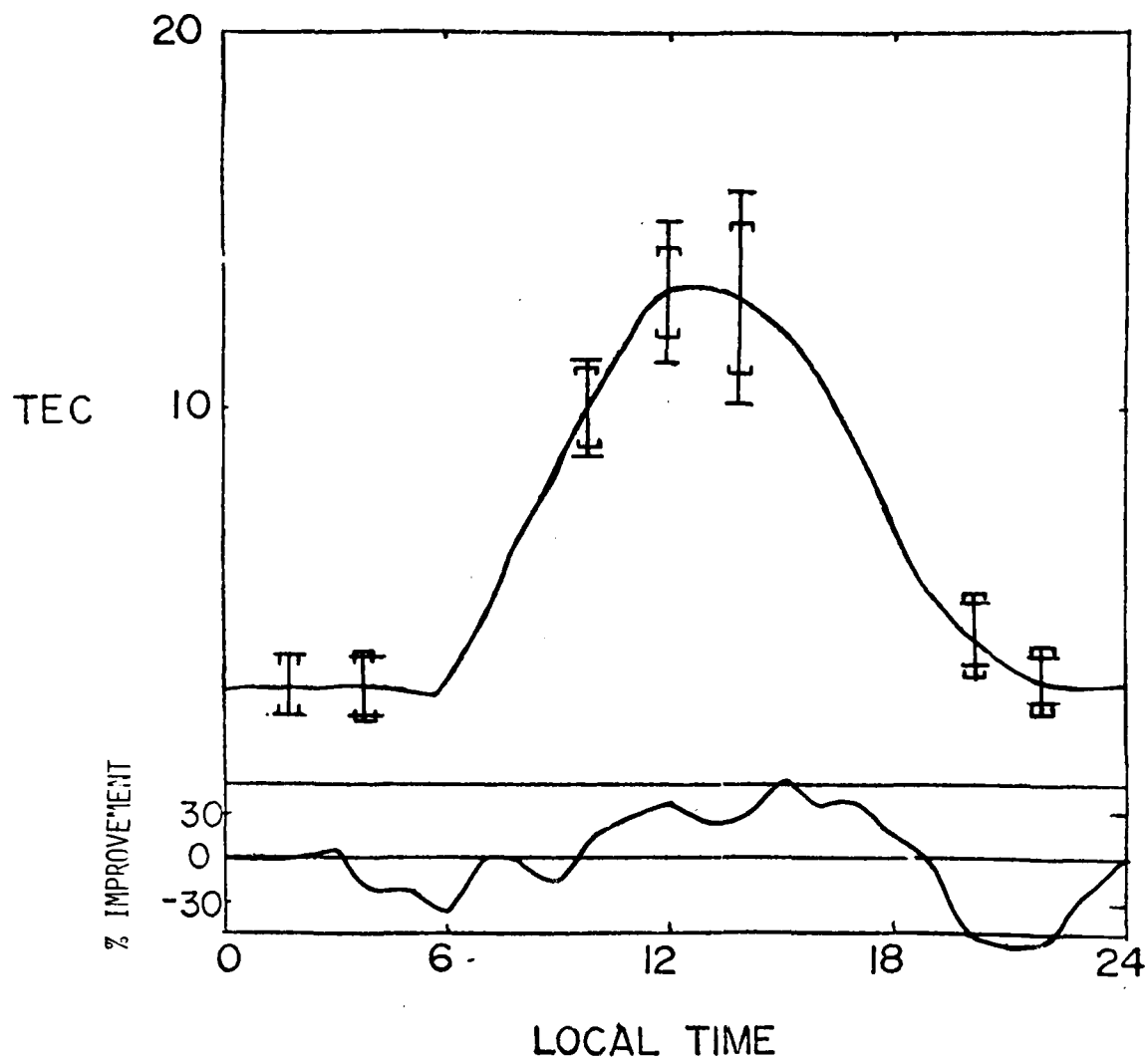


FIG. 20 Same as Figure 16 but using method 5.1b.

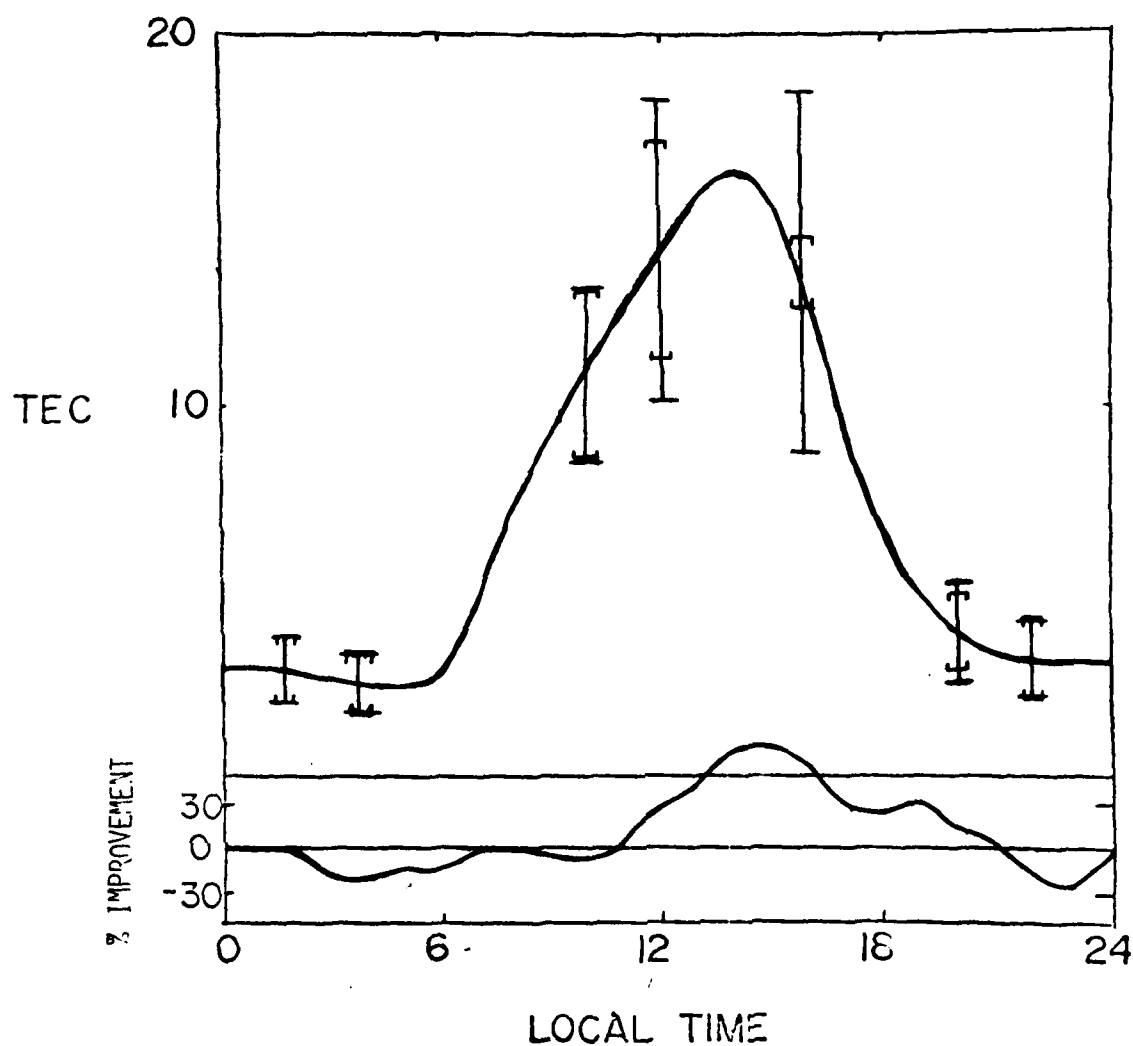


FIG. 21 Same as Figure 17 but using method 5.1b.

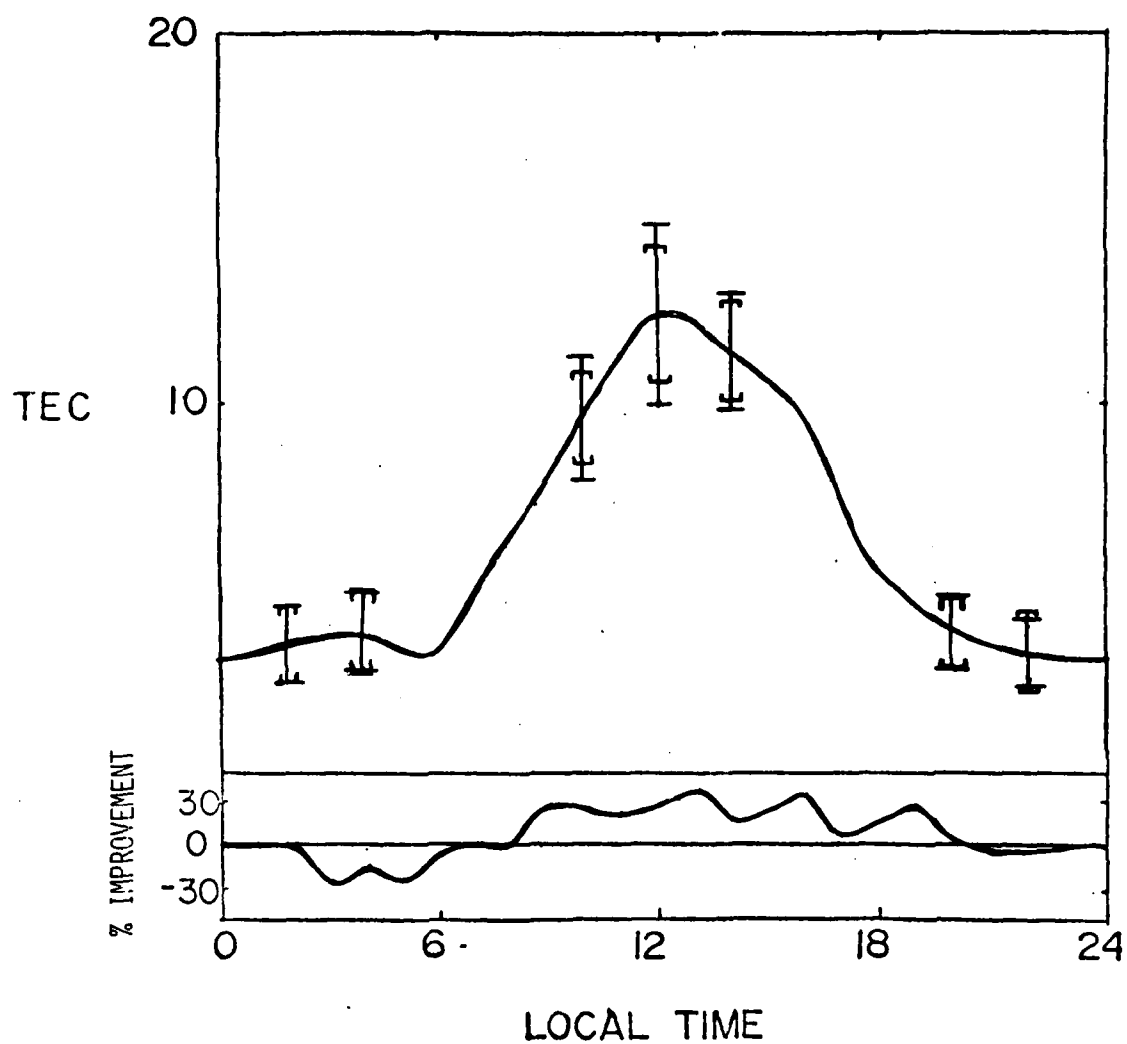


FIG. 22 Same as Figure 18 but using method 5.1b.

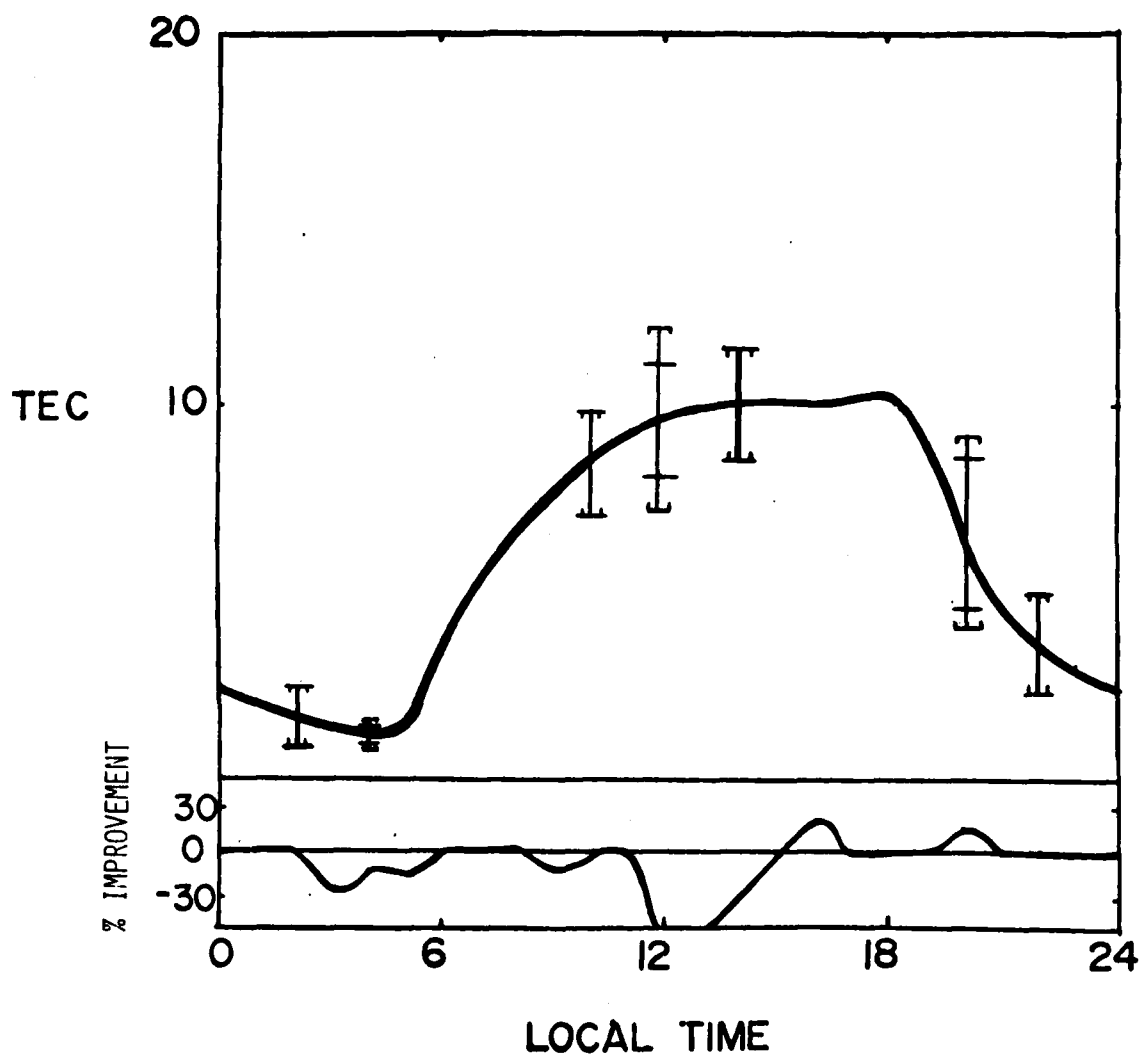


FIG. 23 Average TEC for September, 1975 (as in Figure 19) but using Goose Bay as station B rather than Hamilton/Sagamore Hill. As one can see, no improvement results.

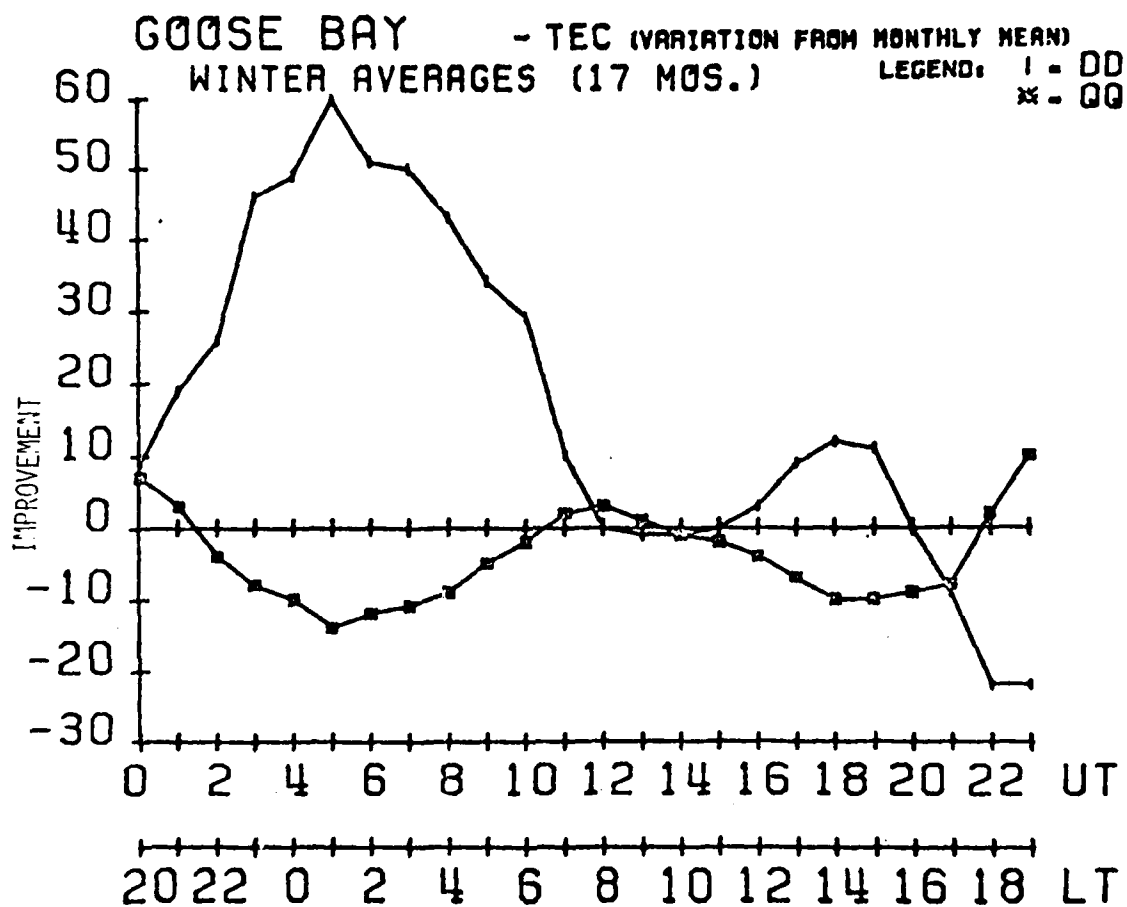


FIG. 24 Average winter diurnal behavior of TEC (%) for the QQ-days and DD-days at Goose Bay for 1974-1976. Note the dissimilar appearance of this to Figure 14 and the minimal response during daylight hours.

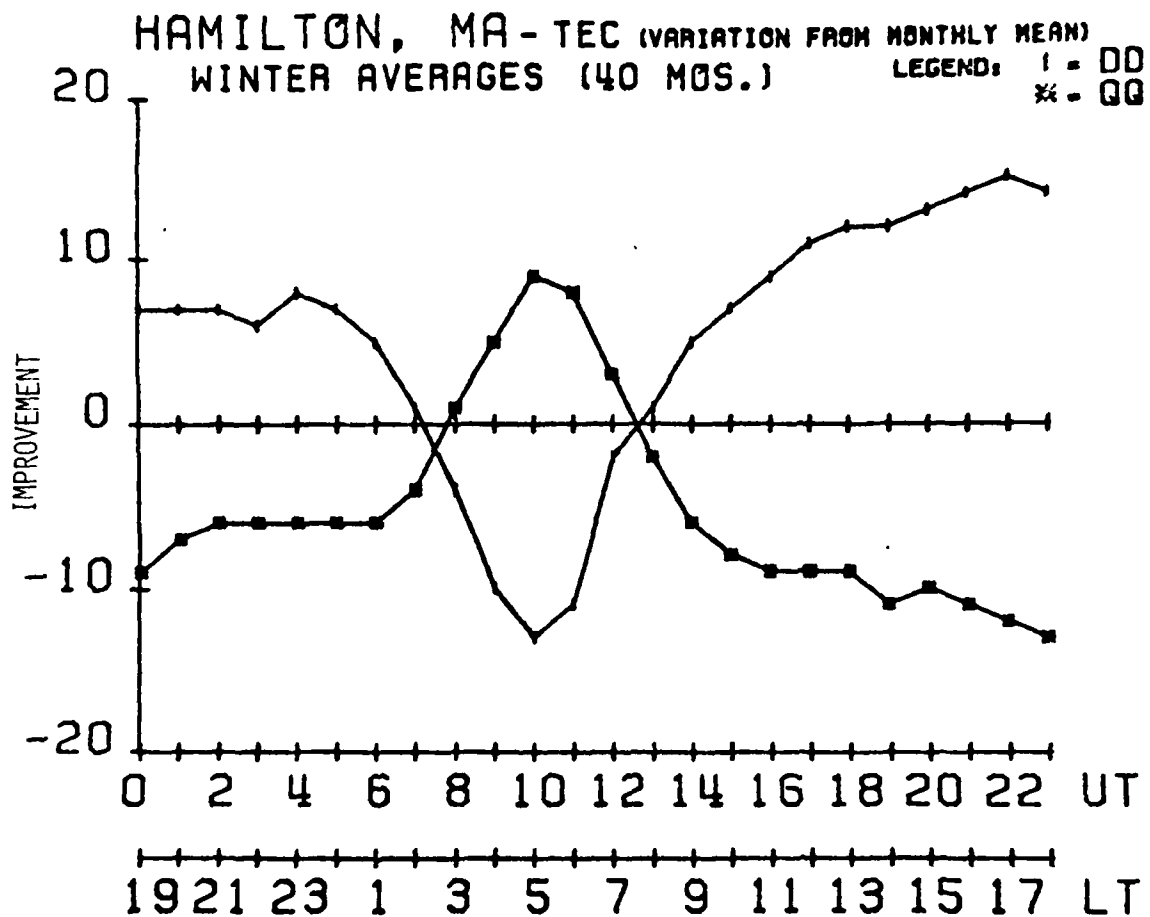


FIG. 25 Average winter diurnal behavior of TEC (%) for the QQ-days and DD-days at Hamilton, MA. Hamilton has a similar response to geomagnetism as KSFC.

He states the correlation coefficient at 2000 km north-south is about the same as 4000 km east-west. Klobuchar and Johanson (1977), using a network of TEC observing stations, reached similar conclusions. It is important to note, however, that "spatial correlation" results are directly associated with the geomagnetic ordering techniques described here. Thus, part of the spatial coherence is due to spatial coherence of geomagnetically induced F-region variations. Previous results giving improved east-west correlations (vs. north-south) support the geomagnetic (rather than solely spatial) dependence in that storm effects are best ordered by geomagnetic latitudes (Mendillo and Klobuchar, 1979).

6. SOLAR RELATED IONOSPHERIC VARIABILITY

Section 5 dealt with geomagnetically induced variability. Insofar as geomagnetic variability is related to solar wind influences (see Akasofu, 1975), part of the solar ionospheric variability would be caused through that agent. Other solar inducing agents that have been suggested are Interplanetary Magnetic Field (IMF) sector boundaries (see Zevakina and Lavrova, 1980) and solar 27-day variability in the ionizing flux associated with spatial structures on the sun (active regions) rotating with this period.

The findings of Zevakina and Lavrova were investigated using a superposed (Chree) analysis of daytime average TEC variations about sector boundaries for 1975 and 1976. In 1975, little overall effect was found about all boundaries, and the only apparent possible effect was an increase by 8% in TEC following +/- sector boundaries listed by Svalgaard(1976). Specifically, 31 "clearly defined" sector boundaries during 1975 were employed; the average daytime (hours 0900-1700) TEC at Hamilton Base was 10.7 (TEC units) for the 5 preceeding days prior to these crossings, 11.5 for the 5 days following these crossings, and 11.0 on the day of these crossings. Although the effect superficially appears significant, it is still required to ascertain whether it is real or possibly related to known yearly sector variations associated with the geometry of the current sheet, or due to statistically related effects.

The significance was assessed in the following way. The 1974 sector boundaries were employed to see whether the effect would "repeat" with earlier data; that is, using 1973 TEC data. The effect disappeared under such tests. The statistics of the 1975 effect were examined as follows: the standard deviation of the daily means was 3.6 TEC units, and only 14 of the 31 boundaries

in 1975 were \pm boundaries. Therefore, the average before the \pm boundary (10.7 TEC units) was uncertain by the "error of the mean" = $3.6 / \sqrt{14-1} \approx 1$ TEC unit. Similarly, the average (11.5 TEC units) after the boundary was approximately this uncertain. Therefore, due to the limited number of boundaries examined, the effect is not yet considered to be statistically significant. A more complete analysis will be carried out during 1980.

A more direct explanation of the solar activity/ionospheric variability is related to 27 days induced spectral irradiance variability. As the ionosphere responds markedly to the 11-year solar variability, if a 27-day spectral variability exists, the ionosphere should respond similarly (considering the short time response of the ionosphere to both these periods). Heath (1973) finds a 27-day UV wavelength dependence variability (in 1969) of about 25% at $L \alpha$ (1216 Å) and a few percent at longer wavelengths. Solar rotational variability of activity parameters is not as great as the general 11-year variability, but it could still (and probably does) play the major role in the 27-day component of ionospheric variability.

A sample study of a direct solar activity/TEC relation was obtained using Lockheed X-ray observations (2-14kV). The noon KSFC observations of TEC during December 1976, were related to the Lockheed solar activity observations. The data were broken into "quiet" or "active" days on the basis of whether the X-ray flux index was less than or greater than 4 Lockheed units (roughly dividing the data during this interval in half). The mean noon TEC value for the quiet data was 9.7 and 10.5 for the active data. As there were roughly 15 points in each group, the effect is not particularly significant--near the 1σ level. Nevertheless, the fact that it is in the "same direction"

as the general trend in solar activity producing TEC 11-year variability gives reason to direct future studies to this area.

7. SUMMARY AND CONCLUSIONS

Short-term variability in ionospheric TEC has been studied in relation to lunar and solar related influences. A predictive formula for the lunar variability has been obtained. It appears as a best fit to the data available from several U.S. east coasts observatories. Phase differences with other longitudes may be possible, and improvements could be made to better fit global data. Height variations of the ionosphere provide an understanding of vertical drift effects on production and loss processes. A specific study carried out at a mid-latitude site yielded a relation between the height of the F-region (hmF2) and TEC during daytime hours.

Solar induced geomagnetic activity has been related to TEC variability and, for mid-latitudes, a real-time predictive method has been developed which removes at best 50% of the standard deviation.

While a preliminary examination of interplanetary sector related TEC variability failed to provide a statistically significant result, the initial results obtained suggest the need for further investigations. Finally, a modest 1-month case study did suggest that short wavelength (spectral irradiance) variations on the Sun could be related to ionospheric variability.

References

- Akasofu, S. -I., The solar wind-magnetosphere dynamo and the magnetospheric substorm, *Planet. Space Sci.*, 23, 817, 1975.
- Bernhardt, P.A., Separation of lunar and solar periodic effects in data, *J. Geophys. Res.*, 79, 4343, 1974.
- Bernhardt, P.A., Identification of mixing frequency components in ionospheric electron content data by multiplicative homomorphic filtering, *J. Geophys. Res.*, 83, 5212, 1978.
- Bernhardt, P.A., Antoniadis, D.A. and A.V. daRosa, Lunar perturbations in columnar electron content and their interpretation in terms of dynamo electrostatic fields. *J. Geophys. Res.*, 81, 5957, 1976.
- Bradley, P.A., A slide for determining hmF2 directly from ionograms, *J. Atmos. Terr. Phys.*, 37, 687, 1975.
- Chapman, S. and J. Bartels, Geomagnetism, Oxford University Press, Oxford. 1940.
- Hawkins, G.S. and J.A. Klobuchar, Seasonal and diurnal variations in the total electron content of the ionosphere at invariant latitude 54 degrees, AFCRL Tech. Report No. 0294, AFCRL, Bedford, MA, 1974.
- Heath, Donald F., Space observations of the variability of solar irradiance in the near and far ultraviolet, *J. Geophys. Res.*, 78, 2779, 1973.
- Huang, Y.N., Lunar variations of total electron content at Lumpung, *J. Atmos. Terr. Phys.*, 40, 1219, 1978.
- Klobuchar, J.A., Trans-ionospheric propagation report, Proc. Solar-Terr. Predictions Workshop, (ed., R. Donnelly) Vol. II, NOAA, Boulder, CO, 1979.
- Klobuchar, J.A. and J. Johanson, Correlation distance of mean daytime electron content, AFGL Tech. Report No. 0185, DCA #ADA 048117, AFGL, Bedford, MA, 1977.
- Llewellyn, S. and R.B. Bent, Documentation and Description of the Bent ionospheric model, AFCRL-TR-73-0657, Los Angeles, CA, July, 1973.
- Matsushita, S., Lunar tides in the ionosphere, *Hand. Der Physik*, XLIX, 547, 1967.
- Mendillo, M. and J.A. Klobuchar, F-region storm morphologies obtained from satellite radio beacon techniques, Proceedings of the Symposium of the Cospas Satellite Beacon Group, Beacon Satellite Measurements of Plasma-spheric and Ionospheric Properties, Firenze, May 1978.
- Mendillo, M. and F.X. Lynch, The influence of geomagnetic activity on the day-to-day variability of the ionospheric F-region, AFGL Tech. Report No. 0074, AFGL, Bedford, MA, 1979.
- Rishbeth, H. and H. Kohl, Topical questions of ionospheric physics: a working group report, *J. Atmos. Terr. Phys.*, 38, 775, 1976.

- Rishbeth, H., Ganguly, S. and J.C.G. Walker, Field-aligned and field perpendicular velocities in the ionospheric F2-layer, *J. Atmos. Terr. Phys.*, 40, 767, 1978.
- Rishbeth, H. and O. Garriott, Introduction to Ionospheric Physics, Acad. Press, N.Y., 1969.
- Rush, C.M., Improvements in ionospheric forecasting capability, AFCRL Tech. Report No. 0138, AFGL, Bedford, MA 1972.
- Rush, C.M., An ionospheric observation network for use in short-term propagation predictions, *Telecommunications J.*, 43, 544, 1976.
- Svalgaard, L., Interplanetary Sector Structure, Tech. Report SUIPR-648, Stanford University, 1976.
- Zevakina, R.A., and E.V. Lavrona, On the possibility to predict variations in the F2-region parameters as a function of the IMF direction, *Proc. Solar-Terr. Predictions Workshop* (ed., R. Donnelly), Vol. III, NOAA, Boulder, CO, 1980.